Journal of Cleaner Production 575 (2026) 149236

Contents lists available at ScienceDirect

Journal of Cleaner Production

journal homepage: www.elsevier.com/locate/jclepro

Eco-Construction from the sea: assessment of mollusk shells by-products as sustainable building materials

Adriana Calà [a], Marinélia N. Capela [b], Rosanna Leone [c], Simona Colajanni [a], Tiziana Campisi [a], Manfredi Saeli [a,*]

[a] Department of Architecture, University of Palermo, Viale delle Scienze Bld. 8-14, Palermo, 90128, Italy
[b] Department of Materials and Ceramics Engineering, CICECO–Aveiro Institute of Materials, University of Aveiro, Aveiro, 3810-193, Portugal
[c] Department of Engineering, University of Palermo, Viale delle Scienze, Bld. 8, Palermo, 90128, Italy

HIGHLIGHTS

- Mollusks shells can effectively replace sand in mortars mix design.
- Mussel shells reduce strength but enable lightweight and insulating mortars.
- Oyster and clam shells significantly improve mortar mechanical performance.
- Shell-based mortars show lower density and enhanced thermal insulation.
- Durability proved under aging salt cycles and thermal loads.

GRAPHICAL ABSTRACT

ARTICLE INFO

Keywords:
Green bio-composite mortar
Mussel
Clam
Oyster
Waste recycling
Durability
Circular economy

ABSTRACT

This paper describes the development of novel bio-composite mortars made by reusing waste from the fish canning industry, namely mussel, clam, and oyster shells, as recycled aggregates to achieve a complete (100%) replacement of conventional sand. For each shell type, different granulometric fractions (0.00–1.00 mm, 1.00–2.00 mm, 2.00–4.00 mm, and a calibrated 0.00–4.00 mm blend) were investigated. Several waste-based cement mixes were tested and compared with conventional OPC mortar. Chemical-physical properties and the functional and engineering performance of the new bio-composite mortars were evaluated to explore their potential for construction applications. Main results indicated a strong dependence of mortar performance on both shell type and particle size distribution. In particular, oyster- and clam-shell mortars significantly improved the mechanical properties, achieving increases of up to 120% in flexural strength and 60% in compressive strength compared with the reference mortar, whereas mussel-shell formulations generally exhibited lower mechanical performance; opposite behaviours were observed for the mussel shell. Nevertheless, developed mixes were

* Corresponding author.
E-mail address: manfredi.saeli@unipa.it (M. Saeli).

https://doi.org/10.1016/j.jclepro.2026.149236
Received 31 March 2026; Received in revised form 26 July 2026; Accepted 16 August 2026
Available online 24 August 2026

analysed in light of EN 998-1 and EN 998-2, for plastering and masonry application respectively, demonstrating potentials for uses in construction, including ordinary and lightweight structures and plasters. In addition, with an average 30% reduction in bulk density and a 40% increase in energy behaviour, the bio-composite mortars resulted particularly suitable for improved energy-saving applications.

Finally, accelerated aging tests based on salt (4% NaCl) crystallization and exposure to high thermal loads (up to 800 °C), permitted to simulate exposure to prolonged stress and preliminary investigate the evolution of degradation phenomena, suggesting long life span. In conclusion, the use of sole bio-waste aggregate offers a sustainable alternative to conventional landfill disposal of the waste and makes these mortars promising candidates for Minimum Environmental Criteria certification, in line with the European Green Deal and Circular Economy principles.

1. Introduction

The construction sector represents a main challenge in the context of environmental sustainability due to the massive use of non-renewable raw materials and significant energy consumption. This situation has led to a growing interest in the development of more ecological practices and materials, within an increasingly strict regulatory framework. The intensive use of natural resources in construction causes significant environmental impact, including resource depletion and greenhouse gas emissions (Naji and Elsheikh, 2023; United Nations Environment Programme, 2023). Most of the materials used, such as cement, steel, and chemical compounds, require large amounts of energy for their production, which increases the industrial ecological footprint (Ghaffar et al., 2018). This dependence on non-renewable raw materials raises critical issues for long-term sustainability and environmental resilience.

In response to these challenges, numerous international regulations and guidelines have been introduced to promote sustainability in construction. Among these, the European Green Deal (European Parliament, 2024) and the United Nations Agenda 2030 (United Nations, 2015) represent two key pillars. The former aims to make Europe the first climate neutral continent by 2050 by promoting the use of clean technologies and the adoption of sustainable practices in all economic sectors, including construction.The Agenda 2030, through its 17 Sustainable Development Goals (SDGs), places special emphasis on innovation and sustainable infrastructure.

In addition, with a view to the Circular Economy (CE), the construction sector must focus on the development of more environmentally friendly and high-performance materials. This includes improving the use of secondary resources, such as recycled materials and by-products, and promoting waste incorporation into manufacturing processes (Tam and Tam, 2006). Implementing sustainable, cost-effective, and greener production processes is nowadays essential to reduce the industrial overall footprint and contribute to global SDGs (Cintura et al., 2021).

At the same time, the rapid growth of the world population has led to an exponential increase in the demand for food and energy resources, accelerating the industrialisation and modernisation of agri-food industries. This development has increased production and improved product quality, but has also resulted in the production of huge amounts of agri-industrial waste, which is often disposed of in landfills (Tsang et al., 2019). According to the United Nations Environment Programme (UNEP), global food waste reached approximately 1.05 billion tonnes in 2022, corresponding to nearly 19% of the food available to consumers worldwide (United Nations Environment Programme, 2024). This situation creates significant treatment and disposal issues, as well as economic losses, and pollutant emissions. To address these challenges, it is essential to develop greener and more sustainable production processes and materials, and promote waste reuse and recycling practices. Sustainable production process design and careful product life-cycle management are key actions for an improved CE (European Council of the European Union, 2024).

Therefore, this paper aims to explore the possibility of reusing and valorising waste for the manufacture of green bio-composite materials for application in construction. More particularly, the considered waste derived from a local fish industry and consisted in the shells of mussels (MS), clams (CS), and oysters (OS). In this work, such waste was pre-treated and reused as sole aggregate to totally replace the standard (commercial) siliceous sand in the manufacture of innovative green bio-composite mortars. That approach would preserve sand in the production of more environmentally friendly OPC-based mortars, in line with the CE approach. Currently, the management of waste from the food industry represents a significant problem globally. Therefore, an alternative solution that allows for more sustainable disposal systems than common landfill or transfer to the sea is needed in order to preserve the environment, reduce waste generation, and fight climate change.

The remainder of this paper is organised as follows: Section 2 presents the waste analysis and literature review; Section 3 describes the materials and the experimental methods used to develop the bio-composite mortars; Section 4 discusses the main results and engineering performance, while Section 5 provides a preliminary evaluation of durability, before the study is concluded in Section 6.

2. Waste origin analysis and literature review

In this work, novel bio-composite mortars were manufactured by upcycling mollusks shells deriving from a fish canning industry. More particularly, waste shells were reused as secondary source aggregate in complete substitution to sand in the manufacture of innovative OPC-based mortars. MS are derived from *Mytilus galloprovincialis* (Fig. 1A) treatment; CS from *Ruditapes decussatus* (Fig. 1B), and OS from *Ostrea edulis* (Fig. 1C). These are common species usually found in the Mediterranean basin or farmed for food purposes.

The production of bivalve mollusks, schematically shown in Fig. 2, is carried out through various marine aquaculture techniques, which vary depending on the species farmed and the environmental conditions. Among these, long-line, raft culture and rack culture systems are widely employed for mussel farming (*Mytilus galloprovincialis*), whereas other species, such as clams and oysters, may also be cultivated in sedimentary environments or using rigid support systems (Gosling, 2015; Smaal et al., 2019; FAO, 2022). The production cycle begins with the collection of seed, which may occur either through natural spat settlement on submerged collectors or via sourcing from other areas. The seed is subsequently placed into tubular nets (seed tubing) and attached to ropes or supporting structures, where the growth phase takes place. During this stage, molluscs develop by filtering phytoplankton from seawater, without the need for external feeding, making this system particularly efficient and environmentally sustainable (FAO, 2022). During the growth phase, molluscs may undergo thinning and declumping operations, which are necessary to ensure uniform distribution and to promote optimal development. Once the commercial size is reached, the mollusks are harvested and transferred to processing facilities, where they undergo cleaning, grading, and depuration processes aimed at ensuring food safety (FAO, 2022). Subsequently, mollusks may be marketed as fresh products or subjected to further processing, such as sterilisation and packaging. Throughout these stages, the separation of the edible fraction results in the generation of significant quantities of shells, which represent a substantial proportion of the total biomass (Yao et al., 2014; FAO, 2024).

Among the food industries, mollusk production is increasing worldwide. This sector is mainly dominated by several Asian countries, with China standing out as the leading global producer (European Market Observatory for Fisheries, 2025). In Europe, mollusk production is significant, with some countries emerging as leaders in the production of mussels, clams, and oysters (European Market Observatory for Fisheries, 2025). With regard to mussels, Spain is the largest European producer, with an annual production of approximately 250,000 tonnes, mainly from the Galicia region (European Market Observatory for Fisheries and Aquaculture Products (EUMOFA), 2022a). As for clams, Italy is the leading European producer, with around 40,000–50,000 tonnes per year, with Adriatic regions such as Veneto, Emilia-Romagna and Marche dominating the market (European Market Observatory for Fisheries, 2025). Regarding oysters, France is the European leader, with an annual production ranging between approximately 120,000 and 150,000 tonnes, mainly concentrated along the Atlantic coast and in Normandy (European Market Observatory for Fisheries and Aquaculture Products (EUMOFA), 2022b).

The growing production of mollusks (for food purposes, e.g. can, restaurant, etc.) inevitably generates a considerable amount of waste, mainly in the form of shells. It has been estimated that processing 1 kg of mollusks produces between 370 g and 700 g of shell waste (Yao et al., 2014). In many cases, however, the management of this waste is not adequately regulated, with the risk of generating environmental impacts such as bad odours, visual pollution, and contamination of the surrounding area due to the decomposition of residual organic matter (Chen et al., 2023). However, as mollusk shells consist mainly of calcium carbonate ($CaCO_3$) (Lertwattanaruk et al., 2012; Silva et al., 2019; Leone et al., 2023), they represent a potential resource rather than mere waste. For this reason, shells are considered a viable secondary resource with the potential to be valorised and turned into raw material for various applications, especially in the construction sector.

In Europe, the management of these materials is regulated by Regulation (EC) No. 1069/2009 (European Parliament and Council, 2009), which governs animal by-products not intended for human consumption. Uncontaminated shells from fish processing fall into category 3, i.e. by-products with a low health risk, which theoretically allows them to be reused in agriculture or industry (European Parliament and Council, 2009). However, in practice, landfill disposal remains the most common method in European countries, resulting in high costs and environmental issues mainly linked to the presence of organic residues that, decomposing, could represent a huge problem for the environment and humans/animals (Chen et al., 2023). In light of these critical issues, the reuse of mollusk shells as a secondary raw material, i.e. in building mortars, is a viable and sustainable solution, in line with the principles of the CE.

In the scientific literature, mollusk shells are usually reported in combination with other waste materials, for the production of concrete, cementitious, and lime mortars. For example, Ez-zaki et al. (2018) explored the partial replacement of sand with MS powder in cement mortars (20%, 40%, and 60 wt%), observing that a 40% substitution offered the highest volumetric heat capacity, while leading to a compressive strength reduction. Chen et al. (2023) investigated the effect of the combined use of MS aggregates and recycled concrete, showing that increasing the percentage of MS both compressive and tensile strength diminished, as well as reducing the corrosion resistance of steel. In addition, the inclusion of MS increased the presence of macropores and general porosity, compromising the mechanical properties and durability of the material. Despite these limitations, Martínez-García et al. (2020) demonstrated that MS has shown promise as building insulating material. Indeed, they showed a thermal conductivity of 0.17 W/m·K, close to the values required for appropriate insulation (0.10 W/m·K) and offer good acoustic performance, especially at low frequencies (100-500 Hz). A previous study by the authors, Leone et al. (2023), highlighted the possibility of producing sustainable bio-composite mortars by completely replacing sand with ground MS. The resulting mortars showed lower thermal conductivity than traditional mortars, with a reduction of up to 50%. In addition, in Martínez-García et al. (2021) MS were used as as loose-fill insulation for the building envelope and as aggregate in mortars and concrete, reducing primary energy consumption by 28.3% compared to standard models. In Lertwattanaruk et al. (2012), MS, CS, and OS grounded shells were reused as cement substitutes up to 20 wt% to develop a cementitious product for masonry and plastering. This incorporation resulted in mortars reduced water requirements and extended setting times, which are advantages for plastering and rendering in hot climates, while also producing adequate strength, lower drying shrinkage, and a reduction in thermal conductivity of 1–45% compared to conventional cement mortars. In Liao et al. (2022) calcined OS powder was used to partially replace cement in mortars, with an increase in flexural strength of 15.28% at 3 days of curing and compressive strength of 22.23% at 7 days. Furthermore, Chen et al. (2020) conducted shear tests on masonry reinforced with modified OS shell ash-based mortars that showed a 122% increase in shear strength compared to unreinforced specimens.

Mollusk shells have also been tested as fillers for other applications, such as in asphalt mixtures. Some studies showed that the inclusion of bio-fillers derived from bivalve shells did not lead to significant discrepancies in mechanical performance compared to traditional limestone fillers, confirming the feasibility of their use in road applications also (Caroscio et al., 2024; De Pascale et al., 2024; Islam et al., 2015). More recently, González-Caro et al. (2025) investigated the incorporation of ground mollusk shells (*Acanthocardia tuberculata*) as a replacement for natural sand in self-compacting cementitious mortars. The authors reported that shell-derived aggregates modified the pore structure and water transport properties of the composites, while maintaining

Fig. 1. Representative mollusk species considered in this study: (A) *Mytilus galloprovincialis* (MS), (B) *Ruditapes decussatus* (CS), and (C) *Ostrea edulis* (OS) (European Commission, 2024).

satisfactory mechanical performance. Their results highlighted the important role played by shell morphology, particle distribution, and calcium carbonate-rich composition in governing the behaviour of the resulting mortars, further confirming the potential of shell waste as a sustainable alternative to conventional mineral aggregates.

To provide a clearer context for this study in relation to the current state of the art, Table 1 presents a comparison of the main studies in the literature concerning the reuse of shellfish shells in building materials.

Overall, the scientific literature suggests that mollusk shells have good potential as construction materials, especially when used as fine fillers or partial substitutes in cementitious products. However, at the best of the authors knowledge, most existing studies have focused on partial replacement levels, single shell species, or specific engineering applications, while durability aspects remain relatively unexplored.

As highlighted in Table 1, the novelty of the present study lies on the investigation of the complete replacement (100%) of natural sand with three different types of mollusk shell waste (MS, CS, and OS), providing a comprehensive evaluation of the physical, mechanical, and thermal performance of the developed waste-based mortars. In addition, the influence of different particle size distributions was systematically assessed with the aim of identifying optimized formulations and better understanding their effect on the final properties of the developed mortars. Moreover, a preliminary assessment of the durability was also conducted. That is sligtly investigated in the existing literature and, usually, when performed, only a few conditions are tested. In this study, along with the complete structural, performance, and functional properties, the contingent evaluation of the durability allowed to predict possible real applications making it possible to consider an effective industrial scaling up and the development of efficaceous building materials.

Overall, the provided results contribute to expand the current scientific and technological knowledge on shell-based construction materials and provide useful information for the valorisation of mollusk shell waste within circular economy strategies and resource-efficient construction practices.

3. Material and methods

3.1. Materials

In this work, the novel green bio-composite mortars were produced using an Ordinary Portland Cement (OPC) as conventional binder, while MS, CS, and OS shells were reused as aggregate in complete substitution to the traditional commercial sand. In detail, the used raw materials were:

- OPC, branded i.work Tecnocem 32.5 R (CEM II/B-LL) by Italcementi (CE marked in compliance with UNI EN 197-1:2011) (UNI EN 197-1, 2011) was selected as reference binder;
- natural siliceous sand by Axton, with a calibrated 0.00–4.00 mm particle size distribution and CE-certified according with UNI EN 13139:2013 (UNI EN 13139, 2013), was used as benchmark aggregate;
- MS, CS, and OS collected as shells waste, deriving from a local fish canning industry, were reused as fine aggregate (0.00–4.00 mm, and fractions) in complete substitution to sand. Despite the local origin, shells composition is mainly made of calcium carbonate ($CaCO_3$, generally in the form of calcite and aragonite) regardless of the geographical origin making the study highly reproducible with analogous mollusk deriving from other geographical areas with

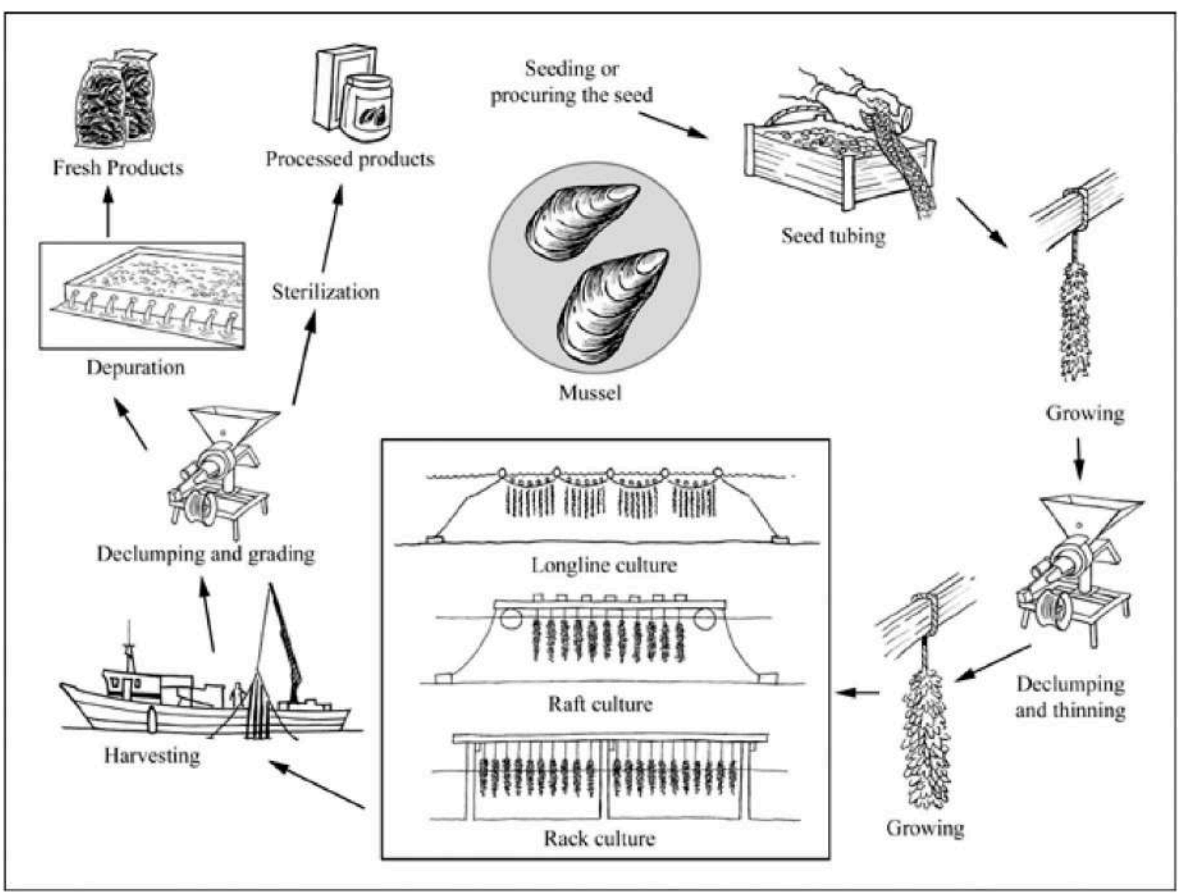

Fig. 2. Schematic representation of the mussel production process, including seeding, growing, harvesting, and processing stages, as well as the main aquaculture systems (long-line, raft, and rack culture). This process is analogous for the other considered mollusks (FAO, 2022).

Table 1
Comparative overview of previous studies on the reuse of mollusk shell waste in construction materials and the main contributions of the present study.

Ref.	Shell type	Material	Replacement strategy	Mechanical properties	Thermal properties	Durability assessment	Full sand replacement
Chen et al. (2023)	MS	Concrete	Partial aggregate replacement	✓	×	✓	×
Lertwattanaruk et al. (2012)	MS, CS, OS	Cement mortars	Partial cement replacement (<20 wt%)	✓	✓	×	×
Silva et al. (2019)	OS	Review/value-added products	Raw material assessment	×	×	×	×
Leone et al. (2023)	MS	OPC mortars	100% aggregate replacement	✓	✓	×	✓
Ez-zaki et al. (2018)	Shell powder	Eco-mortars	Powder incorporation	✓	×	×	×
Martínez-García et al. (2020b)	MS	Insulation materials	Alternative building product	×	✓	×	×
Martínez-García et al. (2021)	MS	Building application	Real-scale assessment	✓	✓	×	×
Liao et al. (2022)	OS powder	Cement-metakaolin mortar	Partial cement replacement	✓	×	✓	×
Chen et al. (2020)	OS ash	Masonry mortar	Mortar modification	✓	×	×	×
Caroscio et al. (2024)	MS, CS, OS	Asphalt concrete	Biofiller replacement	✓	×	×	×
De Pascale et al. (2024)	MS, CS, OS	Porous asphalt	Filler replacement	✓	×	×	×
Islam et al. (2015)	OS	Asphalt mortar	Aggregate replacement	✓	✓	×	×
González-Caro et al. (2025)	*Acanthocardia tuberculata* seashells	Self-compacting mortar	Aggregate replacement (50–100%)	✓	×	✓	✓
Present study	MS, CS, OS	OPC mortars	100% sand replacement	✓	✓	✓	✓

possible very slight variations that do not alter the engineering performance (cf. section "4.1 Waste characterisation") (Lertwattanaruk et al., 2012; Silva et al., 2019; Leone et al., 2023).
- drinkable water, taken from the municipal aqueduct was used in compliance with UNI EN 1008:2003 (UNI EN 1008, 2003);
- releasing agent CS Distak by Gattocel Italia (a natural resin emulsion) was applied to the metallic moulds to ensure easy demoulding and avoid specimens adhesion to the mould surfaces.

3.2. Product mix design

The mix design of the bio-composite mortars was prepared following the standard EN 998–2:2016 (UNI EN 998-2, 2016) adopting a volumetric proportion (V.%) of 1 part of binder, 3 parts of aggregate, and 1 part of water. MS, CS, and OS waste was incorporated in different particle size fractions in compliance with EN 13139:2013 (UNI EN 13139, 2013).

In this work, an OPC-based mortar was prepared as benchmark reference material (Ref. (sand)) for comparative reasons by using a commercial sand (standard granulometry of 0.00-4.00 mm); to reproduce the behaviour of natural sand, MS, CS, and OS shells were ground and sieved into three particle size fractions: 0.00–1.00 mm, 1.00–2.00 mm, and 2.00–4.00 mm. These fractions were investigated individually and compared with the corresponding reference mortars.

In addition, a calibrated 0.00–4.00 mm aggregate was prepared by combining equal proportions of the three granulometric fractions. This approach was adopted to simulate a continuous grading representative of fine aggregates commonly used in masonry mortars. Therefore, the particle size distribution of the calibrated aggregate is directly defined by the composition of the three fractions employed. Images of the resulting aggregate fractions are presented in Fig. 3.

The absence of chemical admixtures was a deliberate experimental choice to exclusively isolate the influence of the aggregate types and granulometry on the novel biocomposite mortars' behaviour, and in light of an improved sustainability. A complete overview of the aggregate composition adopted for each mix is presented in Table 2, together

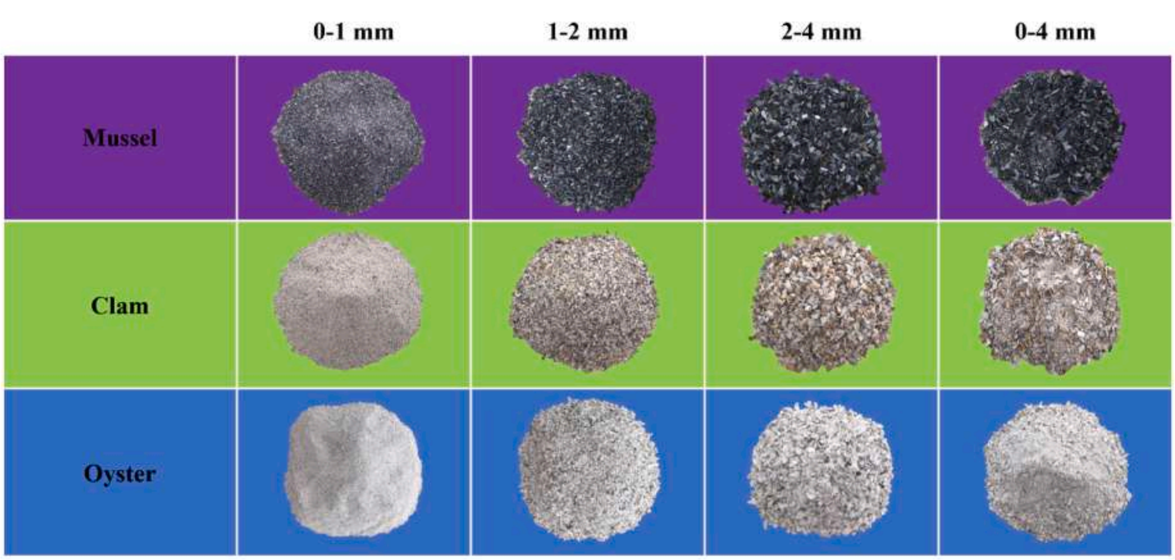

Fig. 3. Visual representation of shell aggregates (MS, CS, and OS) classified by granulometric fractions (0–1 mm, 1–2 mm, 2–4 mm, and 0–4 mm).

Table 2
Experimental plan of the produced bio-mortars.

specimen n.	aggregate nature	granulometric range [mm]	W/B	L/S
1	Ref. (sand)	0.00-4.00	0.714	0.149
2		0.00-1.00		0.153
3		1.00-2.00		0.154
4		2.00-4.00		0.156
5	MS	0.00-4.00		0.178
6		0.00-1.00		0.183
7		1.00-2.00		0.192
8		2.00-4.00		0.201
9	CS	0.00-4.00		0.153
10		0.00-1.00		0.157
11		1.00-2.00		0.173
12		2.00-4.00		0.177
13	OS	0.00-4.00		0.200
14		0.00-1.00		0.237
15		1.00-2.00		0.247
16		2.00-4.00		0.253

with the corresponding Water-to-Binder (W/B) and Liquid-to-Solid (L/S) ratios. Since MS, CS, and OS aggregates exhibit different bulk densities compared to natural sand and among themselves, the mix design was established on a volumetric basis and subsequently converted into mass proportions. A constant volumetric ratio of 1:3:1 (binder:aggregate) and a fixed Water-to-Binder ratio (W/B = 0.714) were adopted for all formulations. Consequently, the Liquid-to-Solid (L/S) ratio varies among the mixtures due to the different aggregate masses required to maintain the same aggregate volume. Therefore, the observed differences in L/S reflect the different densities of the shell aggregates rather than any adjustment of the water content during mixing, ensuring a consistent comparison of their influence on mortar performance.

Finally, each produced mix was tested to investigate the influence of shell aggregate type and particle size distribution on the engineering performance of the mortars. The aim was to evaluate the possibility of producing a homogeneous material and to identify potential applications in the construction sector, according to the relevant standards and guidelines (i.e. EN 998-2 (UNI EN 998-2, 2016), Eurocode 2 (EN, 1992-1-1, 2004), Italian D.M. 17/01/2018 (Italian Ministry of Infrastructure and Transport (MIT), 2018), ACI 116R-00 (ACI 116R-00, 2000), etc.).

3.3. Processing details

Before preparing the mortar mixes, some pre-treatments were implemented on the waste-based aggregate. As received, the MS, CS, and OS shells still contained traces of organic matter and residual salts, and therefore required the following operations:

A) Cleaning: the shells were previously cleaned manually with brushes and sponges up to removing any visible organic residue; subsequently they were washed with running water to remove any traces of dirt and/or remains, as well as the possible sea salt residues;
B) Drying: cleaned shells were then oven-dried at 60 °C for 24 h to eliminate moisture and facilitate subsequent handling and grinding;
C) Grinding: dried shells were initially mechanically fragmented into coarser particles, and then further reduced manually into a ceramic mortar until achieving minute granulometric fractions, generally less than 4.00 mm.
D) Sieving: the sieving phase was carried out using standard metallic sieves, in accordance with UNI EN 13139:2013 (UNI EN 13139, 2013) to obtain the desired selected granulometries (0.00-1.00 mm, 1.00-2.00 mm, 2.00-4.00 mm), useful to analyse - beyond the complete interval 0.00-4.00 mm - the possible influence of the various granulometric ranges in the final mortars performance;
E) Blending: the selected shell fragments' granulometries were mixed to obtain a similar granulometric calibrated range 0.00-4.00 mm of the commercial sand;
F) Packing: the prepared shells granulometries were hermetically packed in a plastic bag to maintain dryness and prevent contamination.

The adopted pre-treatment procedure was developed at laboratory scale. For industrial applications, the cleaning, crushing, and sieving stages could be readily performed using conventional aggregate-processing technologies.

Because the commercial sand contained approximately 12 wt% moisture, it was also oven-dried at 60 °C for 24 h prior to use, cooled naturally, and stored in sealed bags to preserve the designed water/binder ratio.

Mortar preparation followed the procedure described in EN 196–1:2016 (UNI EN 196-1, 2016), and was carried out at laboratory ambient conditions (20 ± 2 °C, 65% RH). The process consisted of simple, safe, reproducible, and sustainable steps. Mixes were produced with a programmable automatic mixer (Automix mod. 65-L0006/AM by Controls). Water, binder, and aggregate were added sequentially, starting by filling the mixer bowl with water and adding, according to the time established by the standard (UNI EN 196-1, 2016), first the cement and finally the aggregate. Standardised mixing speed/time was: i) 140 rpm for 60 s during the raw materials introduction, ii) 285 rpm for 30 s for homogenisations, iii) pause (0 rpm) for 90 s to allow the water to be absorbed by the binder particles, and iv) 285 rpm for 60 s to ensure slurry uniformity up to completion.

Fresh mortars, in accordance with UNI EN 1015–11:2019 (UNI EN 1015-11, 2019), were poured into standard metallic moulds (40 x 40 × 160 mm), previously coated with the release agent. The material was compacted with 25 manual tamping strokes and light vibration to ensure uniform distribution and minimise entrapped air. At the end, the leftover mortar was removed with the aid of a metallic spatula, in order to obtain a flat upper surface, levelled to the mould edge. Once the slurry was carefully poured and set into the standard moulds, specimens were cured, in compliance with the same UNI EN 1015–11:2019 (UNI EN 1015-11, 2019), at ambient conditions by following the next consecutive phases:

1) days 1-2: the moulds - filled with the fluid slurry - were kept closed in plastic bags to grant 95 ± 5% RH;
2) days 3-7: once the slurry was hardened, the specimens were taken out from the moulds (if some specimens still resulted wet/viscous, they were kept in the moulds for other 24 h), put again in the same bags, and kept closed to grant the same curing conditions;
3) day 8: specimens were removed from the bags and stored at ambient laboratory conditions;
4) day 8-28: specimens were cured at ambient conditions until testing.

This curing procedure was adopted in accordance with UNI EN 1015–11:2019 (UNI EN 1015-11, 2019) to ensure adequate hydration and comparable curing conditions for all mortar formulations.

3.4. Materials characterisation

The mineralogical composition of the considered waste aggregates (MS, CS, and OS) was determined by X-ray powder diffraction (XRD) using a θ/θ diffractometer (X'Pert Pro3, Malvern PANalytical) equipped with a fast RTMS detector (PIXcel 1D, Malvern PANalytical). The measurements were taken at room temperature with Cu Kα radiation (45 kV and 40 mA) over a 2θ range of 5-80°, using a virtual step scan of 0.02° and a virtual time per step of 200 s. Phase identification was made using X'Pert High Score Plus PRO3 PANalytical software. For this analysis, samples were ground to a particle size inferior to 63 μm. The chemical composition was evaluated by X-ray fluorescence (XRF) using a Axious PANalytical spectrometer. For this analysis, 10 g of dry and ground (<63 μm) sample (Shan et al., 2008) was homogenized with five drops of polyvinyl alcohol and pressed. The mass loss of ignition (LOI) of the dried samples was also measured (at 1000 °C for 15 min) using a laboratory muffle. True density and specific surface area of the dry and ground (<63 μm) sample were evaluated using a helium pycnometer (Ultrapyc 3000, Anton Paar GmbH) and nitrogen adsorption isotherms using the Brunauer–Emmett–Teller (BET) method (Micromeritics Gemini 2370 V5.00), respectively. Bulk density was calculated as the average of three tests, based on mass and geometric dimensions. Particles morphology was observed by scanning electron microscopy (SEM, SU-70, Hitachi) following coating with a thin carbon film (K950, Emitech) to provide a conducting layer. Additionally, optical images were obtained using a Nikon optical microscope (P-SXY64).

The consistency of the fresh slurry was evaluated through the flow table test in conformity with EN 1015-3:1999 (UNI EN 1015-3, 1999), measuring the slurry spread on an automatic flow table, model 63-L0037/E by Controls. Bulk density and volumetric shrinkage were calculated at 28 days of curing from geometric calculations, as the average of three specimens. Mass loss during curing was evaluated by weighing daily for all the produced specimens from the 8th day (specimens taken out from the plastic bag) to the 28th (curing termination, according to mentioned standards). Given values were the average from weight variations ($\Delta P_{8\text{-}28}/P_8\%$) and return the quantity of water loss due to both natural evaporation and hydration. Microstructural analysis of the mortars was performed using SEM (SU-70, Hitachi) and optical microscopy (P-SXY64, Nikon). The water imbibition (weight variation, $\Delta P/P$ %, where ΔP represents the variation in specimen mass after immersion and P is the initial dry mass) and the capillary index were determined according with EN 1015–18:2004 (UNI EN 1015-18, 2004); prior to testing, specimens were oven-dried at 60 °C for 24 h to reach constant mass. Reported results correspond to the average of three measurements per formulation. Mechanical properties were assessed according with EN 1015–11:2019 (UNI EN 1015-11, 2019) and EN 998-2:2016 (UNI EN 998-2, 2016) using a universal testing machine (Controls mod. Automax 5) equipped with a 250 kN load cell. The Bending Resistance (BR) was determined through a three-point bending test with the cell running at a rate of 0.50 MPa/s, and with a support span of 100 mm; the Uniaxial Compressive Strength (UCS) was measured under uniaxial loading at 0.75 MPa/s. Values represent the mean of three specimens. The thermal conductivity (λ) was measured using an HFM-CT 1000 calorimeter in accordance with UNI EN 12667:2002 (UNI EN 12667, 2002). Specimens were pre-dried at 60 °C for 24 h to remove residual moisture and to ensure comparable testing conditions among all formulations. Therefore, the reported thermal conductivity values refer to dry-state conditions. Three tests were conducted for each mortar mix.

Finally, preliminary durability tests were performed to evaluate the saline attack and the exposure to thermal loads. As far as the saline exposition, specimens were immersed in containers filled with salty water with a NaCl concentration of 4% for 6 h. Afterwards, the specimens were dried in a conventional oven at a temperature of 60 °C for 18 h. This procedure was adapted from accelerated durability protocols commonly adopted in the literature for investigating salt crystallization effects in cementitious materials (Galanaki et al., 2022; Nogueira et al., 2020; Bai et al., 2021). The objective was to perform a comparative assessment of the behaviour of the different mortar formulations under repeated saline exposure and drying conditions. The specific salt concentration in the water was chosen to simulate the average salt content of seawater, which contains approximately 4 wt% soluble salts, consisting about 2% chloride, 1.1% sodium, 0.28% sulphate, 0.14% magnesium, 0.05% calcium, and 0.04% potassium (Galanaki et al., 2022). All the specimens were subjected to a total of 30 test cycles to assess durability to disintegration caused by salt crystallization. During each test cycle, the mass was measured and photos were taken for visual inspection to assess the loss of material or document the formation of efflorescence and cracks.

For the durability test under thermal loads, specimens were transferred into an electric ceramic furnace and subjected to thermal exposure at 100 °C, 200 °C, 400 °C, 600 °C, and 800 °C for 1 h exposure each. Separate specimens were used for each exposure temperature in order to avoid cumulative thermal damage effects. Afterwards, the tested specimens were cooled naturally down to room temperature, and then the mass loss, and UCS were calculated, according with EN 1015-11:2019 (UNI EN 1015-11, 2019).

In all the following Figs. 5–15 the reference cementituious mortar is coloured in orange; the MS-based mortars in purple; the CS-based mortars in green, and the OS-based mortars in blue.

4. Results and discussion

4.1. Waste characterisation

Fig. 4 presents the XRD patterns of MS, CS, and OS. All three samples are composed primarily of the crystalline phases calcite and aragonite, which are two polymorphic forms of calcium carbonate ($CaCO_3$) (Leone et al., 2023; Martínez-García et al., 2020a; Luo et al., 2024; Bhatti et al., 2008; Checa et al., 2007).

In agreement with this, XRF analysis reported CaO as the main oxide component (94.78 wt% for MS, 97.30 wt% for CS, and 87.12 wt% for OS) (Table 3), where CaO represents the conventional oxide equivalent

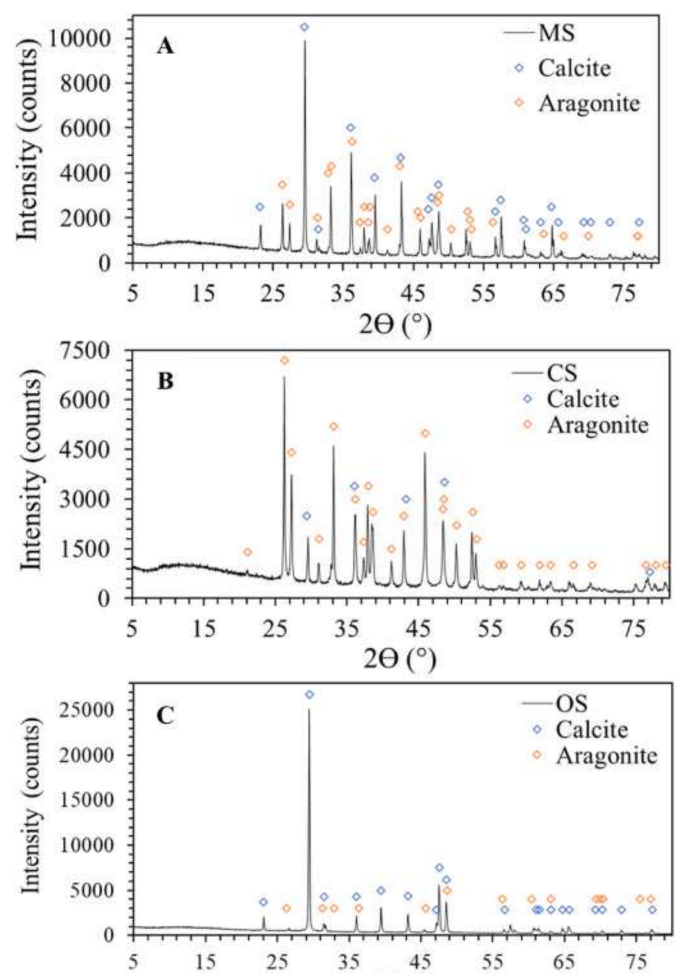

Fig. 4. XRD patterns of: A) MS; B) CS; C) OS.

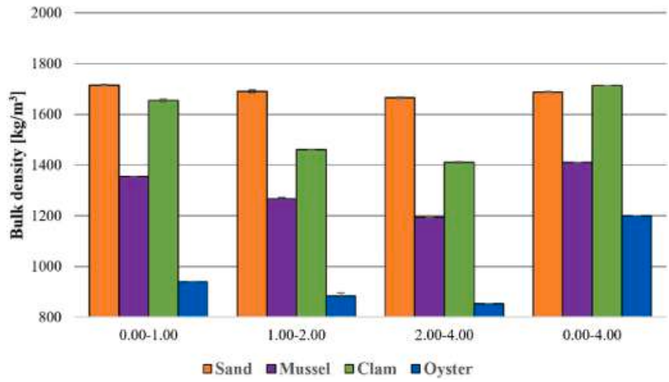

Fig. 5. MS, CS, and OS bulk density compared to that of sand.

of calcium in carbonate form rather than free CaO in the material.

The high loss on ignition (LOI) values (44.91 wt% for MS, 39.51 wt% for CS, and 45.14 wt% for OS) are mainly attributed to the thermal decomposition of $CaCO_3$, with the associated release of CO_2 upon heating, in agreement with previous studies (Yao et al., 2014; Lertwattanaruk et al., 2012; Alonso et al., 2021; Yoon et al., 2003; Harper, 2000; Kobayashi and Samata, 2006; Martínez-García et al., 2017).

The measured specific surface area of the shell samples was 1.73 m^2/g for MS, 3.85 m^2/g for CS, and 21.17 m^2/g for OS, while the reference sand showed a value of 1.72 m^2/g. The true density measured by helium pycnometry for the shell samples resulted 2.64 g/cm^3 for MS, 2.83 g/cm^3 for CS, and 2.65 g/cm^3 for OS, all values comparable to that of the sand, which was 2.70 g/cm^3. The true density results obtained for the shell samples were in line with those reported by De Pascale et al. (2024), despite the use of a different experimental method. The bulk density of the MS, CS, and OS – in the various prepared granulometries - is shown in Fig. 5, and the optical images in Fig. 6. It is observed that, for each type of considered aggregate, both reference (commercial sand) and shell waste, as the particle size increases, the bulk density diminishes. That is due to the larger spaces between larger shells fragments. In comparison, the calibrated 0.00-4.00 mm MS, CS, and OS aggregate presented higher bulk densities as, reasonably, the smaller fractions (0.00-1.00 mm) tend to occupy all the available voids. In any case, OS aggregate resulted much lighter than the commercial sand, except for the CS-calibrated aggregate, which resulted about the same. During crushing, it was also found that, compared to MS and CS, which have a more compact shell, OS were composed of many overlapping layers with different orientations. That generated microvoids between one layer and another, making the material (shell) lighter overall. According with Silva et al. (2019) OS valves structure is composed of a laminated leaf-shaped internal part and a porous external element with a reticular structure, further contributing to the reduced density of the material. Based on the results obtained for both true and bulk density, and considering that the true density values of the four shell types and sand are relatively similar, it is evident that sample packing played a significant role in the bulk density measurements. Additionally, the lower bulk density observed for the OS shell sample can be attributed to the particular structure of the OS shells themselves, as previously discussed.

Optical images (Fig. 6) revealed the morphology of the granulometric fractions of MS (Fig. 6A–C), CS (Fig. 6D–F), OS (Fig. 6G–I), and sand (Fig. 6J–L) in the fractions 0.00–1.00 mm, 1.00–2.00 mm, and 2.00–4.00 mm, respectively. In general, all shell particles exhibited irregular size and shape with sharp edges and angular corners, with MS

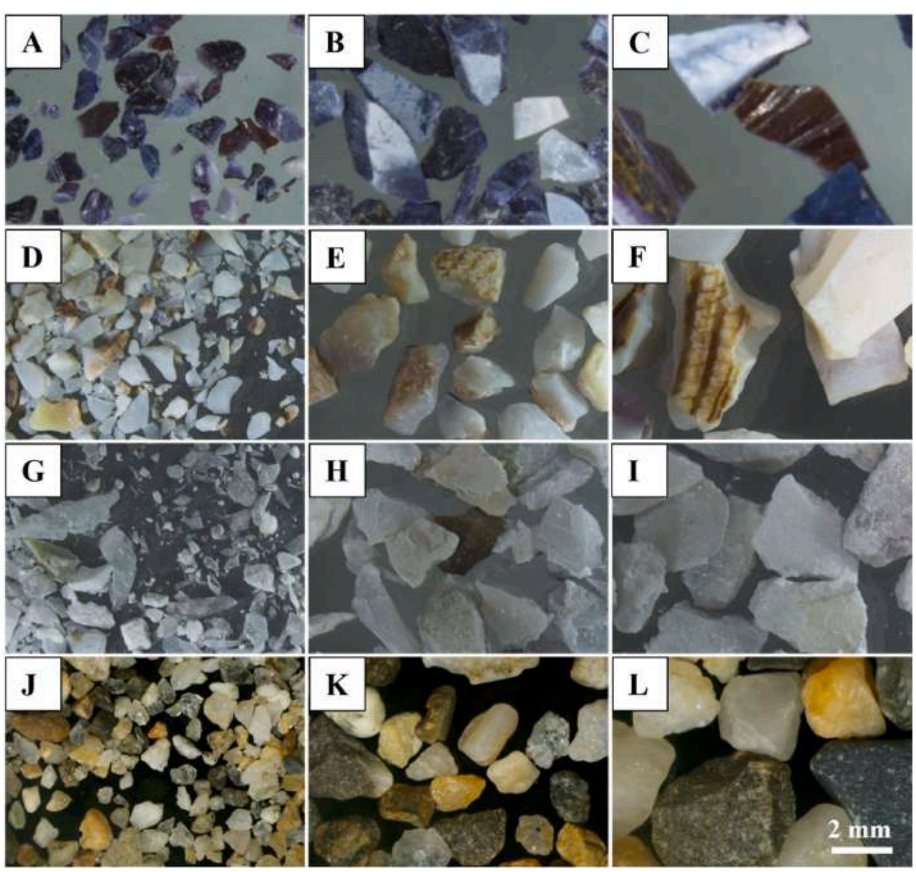

Fig. 6. Optical images: A) MS: 0.00-1.00 mm; B) MS: 1.00-2.00 mm; C) MS: 2.00-4.00 mm, D) CS: 0.00-1.00 mm; E) CS: 1.00-2.00 mm; F) CS: 2.00-4.00 mm; G) OS: 0.00-1.00 mm; H) OS: 1.00-2.00 mm; I) OS: 2.00-4.00 mm.

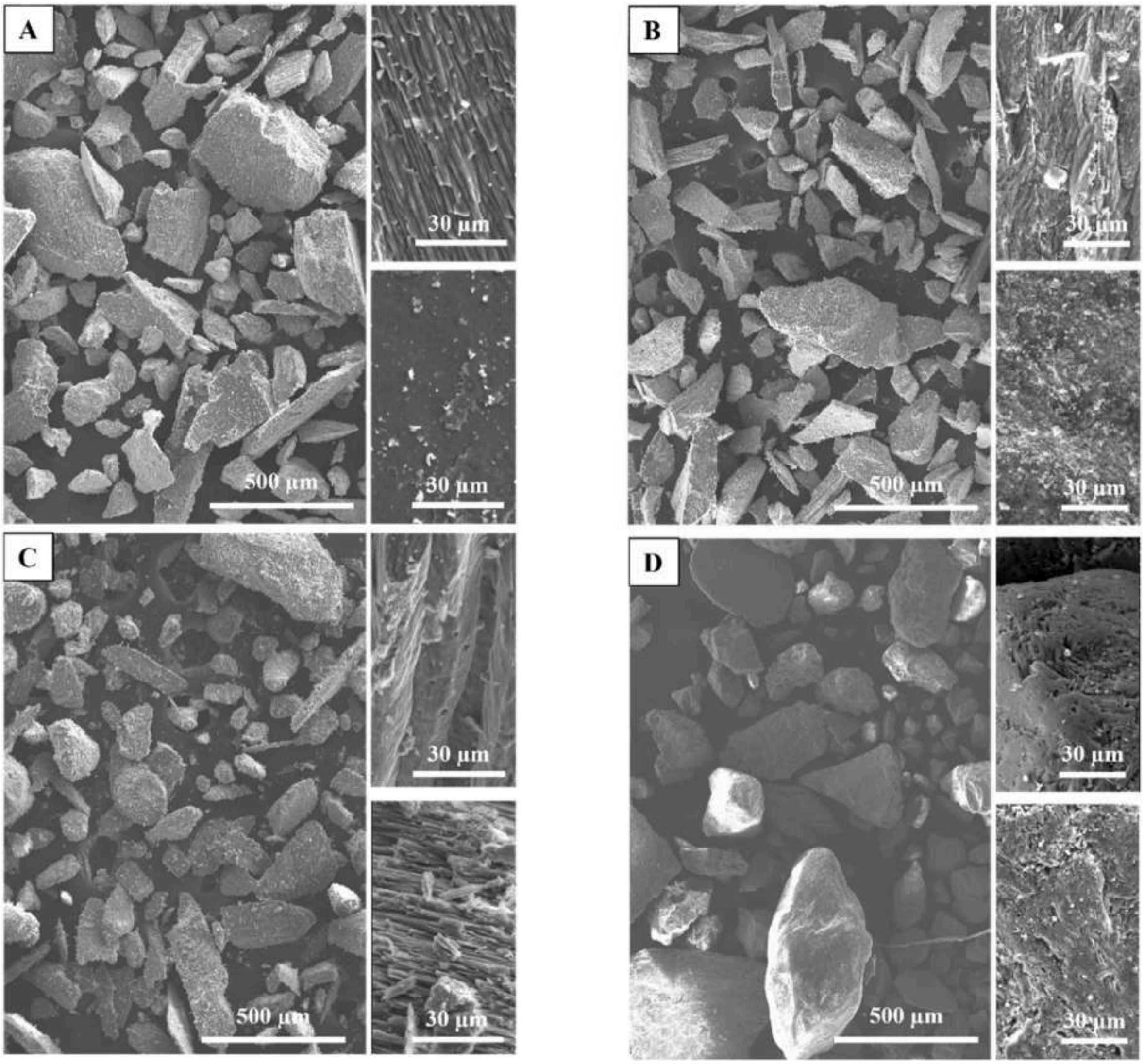

Fig. 7. SEM micrographs of the 0.00–1.00 mm particle fraction of MS (A), CS (B), OS (C), and natural sand (D), highlighting surface features of the different aggregates.

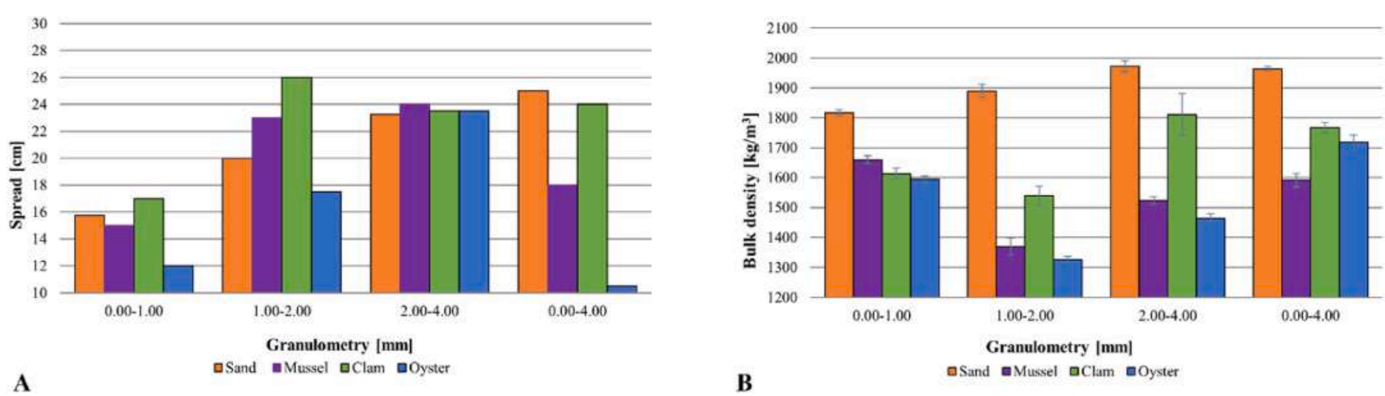

Fig. 8. A) measured spread (workability); B) bulk density.

particles showing a more plate-like morphology. Finer fragments appeared smoother and more rounded. Sand particles tend to show a more equant morphology with reduced angularity compared to the shell particles.

These features are clearly visible in the SEM images of the smaller fraction (0.00–1.00 mm), as shown in Fig. 7, which also reveal that the shell particles exhibit a rougher surface texture than the sand particles, especially the OS sample. This observation is consistent with the specific surface area measurements, as OS showed a much higher specific surface area (21.17 m^2/g) than the other shell samples and the reference sand.

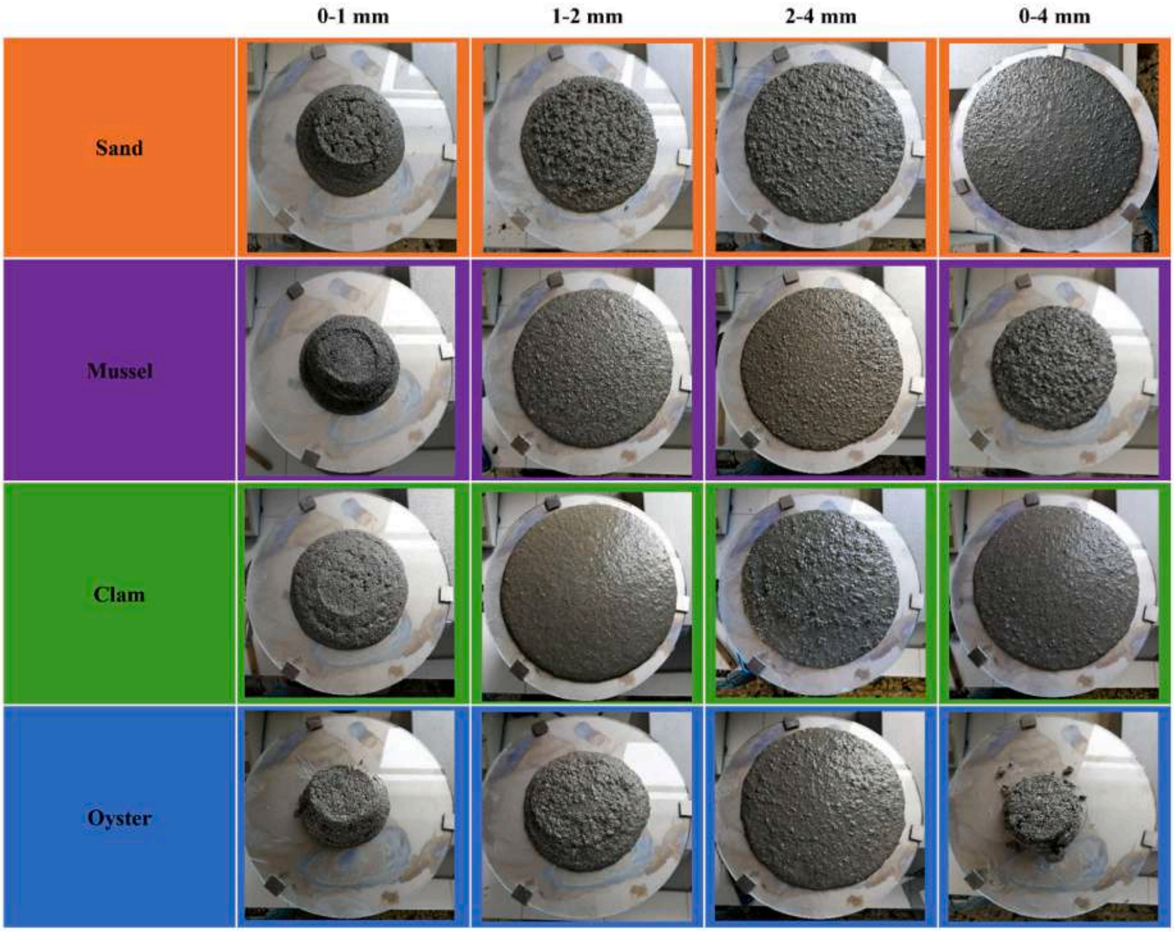

Fig. 9. Spread of mortar samples obtained from flow table test, comparing different aggregates (sand, MS, CS, and OS) and granulometric fractions (0–1 mm, 1–2 mm, 2–4 mm, and 0–4 mm).

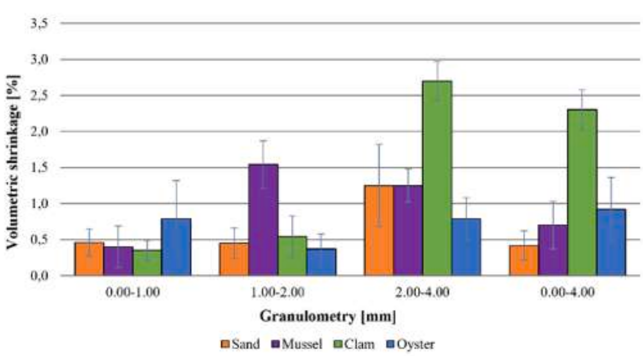

Fig. 10. Volumetric shrinkage.

4.2. Mortars characterisation

The properties of the final mortars are strictly dependent on the adopted mix design, on the characteristics of the raw materials, and on the preparation procedure. All these aspects contribute significantly to obtaining a material suitable for construction purposes, ensuring adequate performance and durability.

Once the features of the waste-derived raw materials were identified, particular care was required in defining the mortar formulations. In fact, an inaccurate mixture may cause difficulties during casting, improper setting, or even premature failure. Conversely, an appropriate mix proportion allows correct blending of the components, effective cohesion between binder and aggregates, and overall uniformity of the hardened product.

4.2.1. Mortars macroscale properties

Figs. 8A and 9 show the workability of the produced mortars; Fig. 8B the measured bulk density. Workability is a key parameter, as it provides an indication of the ease with which the slurry can be mixed and placed without generating defects such as voids or segregation, which may compromise the final mechanical behaviour (Saeli et al., 2019; Dassori and Morbiducci, 2020).

In this study, fresh consistency was evaluated using the flow table test. For typical construction uses, a spread of around 18–22 cm is considered a standard workable range, while significantly lower values indicate a mix that is too stiff, and very higher values denote an overly fluid slurry. No additives were used so that the effect of MS, CS, and OS granulometry on the final workability could be directly assessed.

Although no quantitative analyses were performed to determine the possible presence of residual organic matter on the shell surfaces after cleaning, the adopted washing procedure removed all visible organic residues prior to crushing. Moreover, no abnormal delays in setting or hardening were observed during mortar preparation and curing compared with the reference mixture, suggesting that any residual organic matter, if present, did not produce an evident influence on the hydration process under the investigated conditions.

As expected, the mortars workability was quite reduced by using very thin MS, CS, and OS aggregate (0.00-1.00 mm) as the small particles tend to occupy the paste voids making it pastier. It should also be

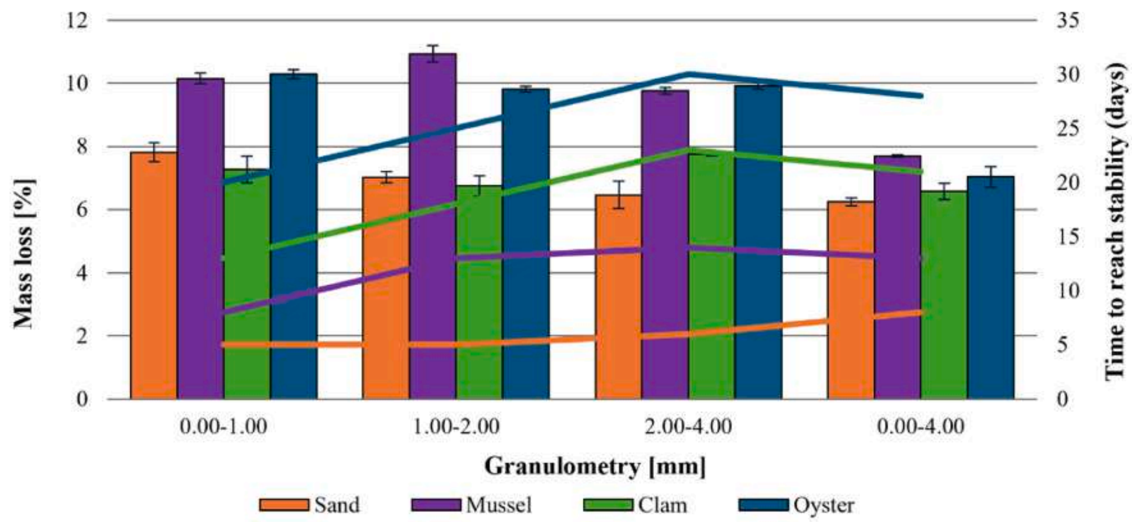

Fig. 11. Mass loss during curing and number of days to reach environmental stability.

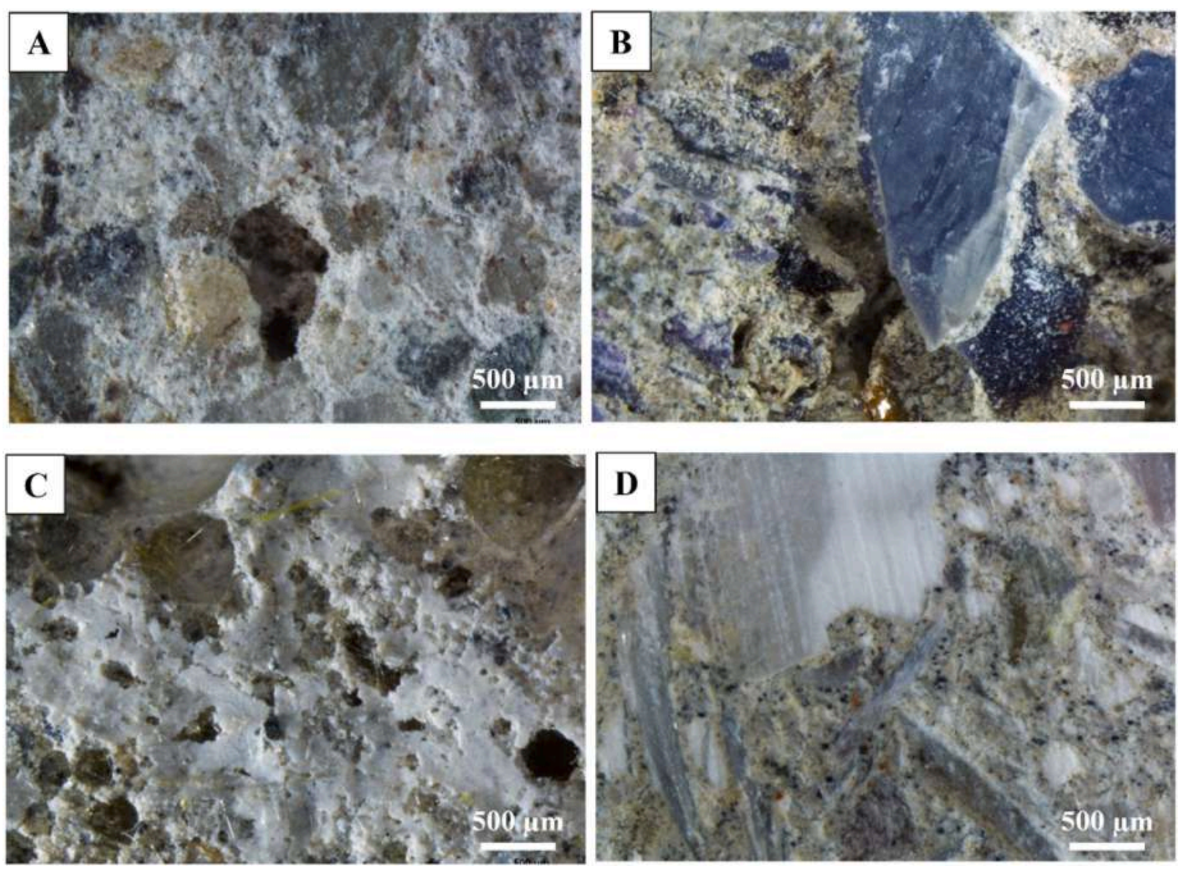

Fig. 12. Optical imaging of sections of cement mortar samples with aggregate particle size fraction 0.00-4.00 mm: A) Sand; B) MS; C) CS; D) OS.

noted that the workability results cannot be attributed solely to aggregate type and particle size distribution. Although a constant Water-to-Binder ratio (W/B = 0.714) was maintained for all formulations, the Liquid-to-Solid (L/S) ratio varied due to the different aggregate densities. Therefore, the trends observed in Fig. 9 reflect the combined influence of aggregate morphology, grading, and mix-design parameters, which may subsequently affect porosity development and mechanical performance. Moreover, the smaller particles need more water to lubricate their surface which diminishes the mixture workability. On the other hand, increasing the MS, CS, and OS granulometry the workability increases. In fact, the opposite behaviour was verified for the 1.00-2.00 mm and 2.00-4.00 mm granulometries, as expected, which increased the mixtures spread. Moreover, the flatness and irregular shape of these particles compromises the compactness of the slurries in the mould, despite the better spread (that resulted from more available kneading water), decreasing their density and consequently higher

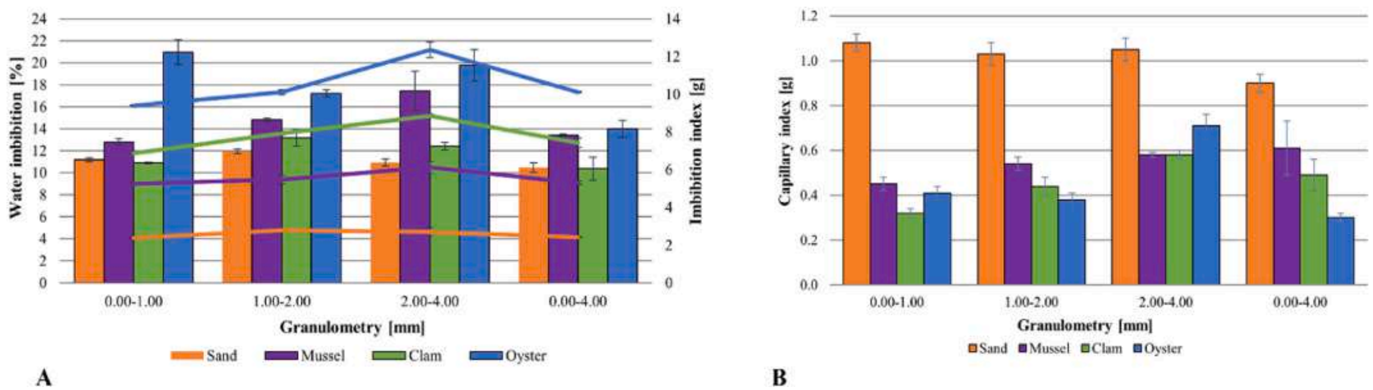

Fig. 13. Water sorptivity: A)water absorption by imbibition, imbibition % and index; B)capillary index.

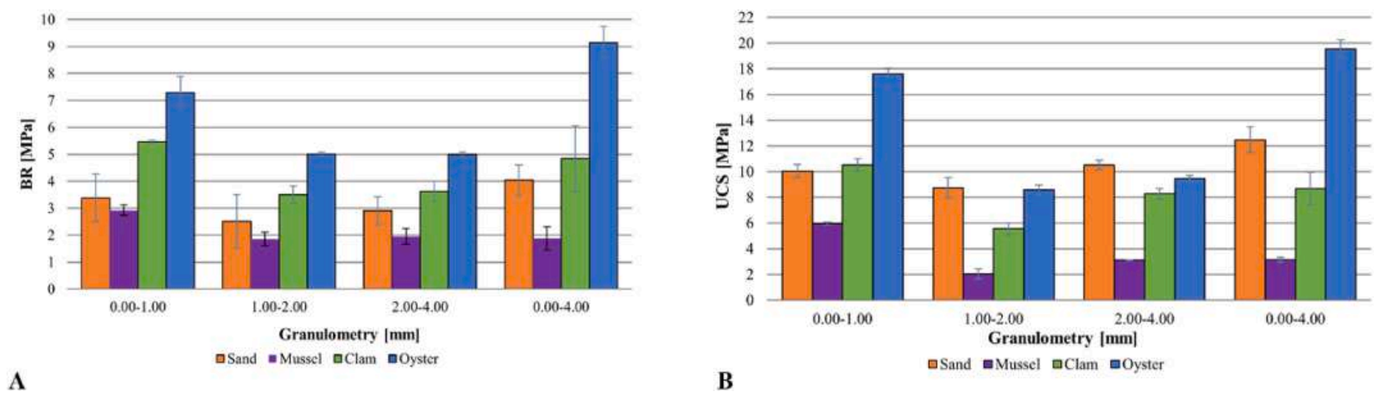

Fig. 14. Mechanical performance of the mortars: A) Bending Resistance (BR); B) Uniaxial Compressive Strength (UCS).

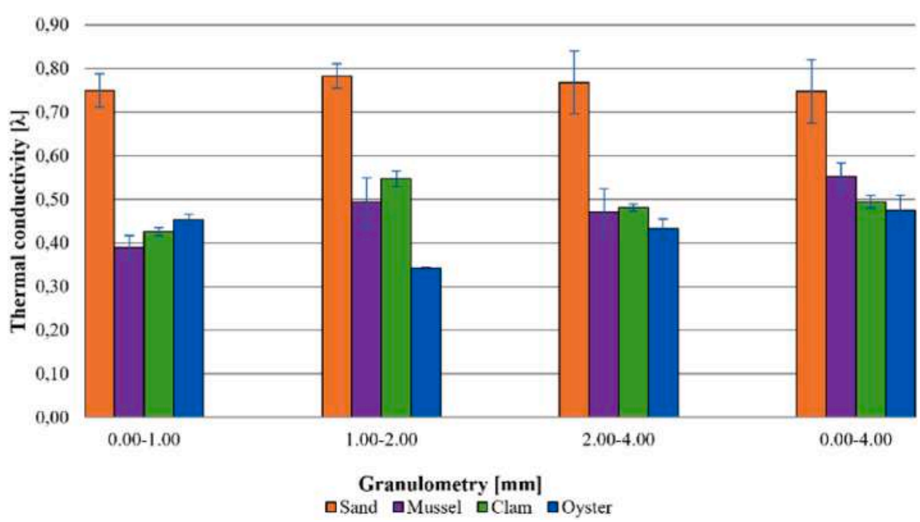

Fig. 15. Thermal conductivity (λ) of the produced mortars.

water absorption. The calibrated CS 0.00-4.00 mm was comparable to that of commercial sand, indicating that the workability of a traditional mortar is similar to the considered waste-based one. That was partially expected as the aggregate granulometric range is one of the major factors affecting such property; here, the CS calibrated 0.00-4.00 mm granulometric range was prepared to simulate the sand's one, hence there is a direct relation between the two. With regard to the MS calibrated 0.00–4.00 mm, the spread value decreased from 25 cm to 18 cm, corresponding to a reduction of approximately 28% compared to the reference mortar with sand aggregate. On the other hand, the workability of the OS calibrated 0.00-4.00 mm showed a significant reduction, with the spread value decreasing drastically to 10.5 cm, making the mix practically unworkable.

Bulk density varied a lot depending on the used mollusks aggregate. Indeed, all the specimens resulted much less dense than the reference mortar, in accordance with the aggregate density that is lighter than the sand (cf. Fig. 5). For example, the reference mortar with a calibrated particle size distribution of 0.00–4.00 mm had an apparent density of

Table 3
MS,CS, and OS chemical composition, as estimated by XRF.

Compound (wt.%)	MS	CS	OS
CaO	94.78	97.30	87.12
SiO_2	1.41	0.41	0.62
Na_2O	1.35	1.10	7.37
SO_3	0.67	0.31	0.75
Cl	0.60	0.05	2.97
MgO	0.54	0.13	0.59
P_2O_5	0.16	0.10	0.20
Al_2O_3	0.16	0.10	0.12
Sr	0.15	0.28	0.12
Fe_2O_3	0.11	0.13	0.06
K_2O	0.03	0.02	0.06

1964 kg/m^3, whilst the corresponding MS-based formulation recorded a value of 1591 kg/m^3, corresponding to a reduction of approximately 19%. Among the shell-based mortars, the samples containing the finest fraction (0.00–1.00 mm) and the calibrated particle size distribution (0.00–4.00 mm) generally exhibited the highest density values. This behaviour can be attributed to the greater ability of fine particles to fill the available voids, resulting in a more compact packing of the matrix despite the mix design being based on constant volumetric proportions.

Fig. 10 shows that volumetric shrinkage increased for the first three particle size fractions. Samples with MS and CS aggregate showed more than 1% shrinkage for the fractions of 1.00-2.00 mm and 2.00-4.00 mm. For the fraction ranging 0.00 to 4.00 mm, the samples with CS aggregate showed higher shrinkage than those with MS and OS aggregate. The differences observed suggest that shrinkage behaviour is influenced by both the nature of the aggregate and the particle size distribution used. This increase in shrinkage may be related to the different water absorption behaviour of aggregates derived from shells, which can affect the availability and redistribution of moisture during the curing phase. Consequently, depending on the type of aggregate and the particle size distribution used, different responses may develop in terms of volumetric shrinkage. A qualitative correlation can also be observed with the mass-loss behaviour, as reported in Fig. 11, since the formulations exhibiting higher water loss during curing generally showed greater shrinkage values. Nevertheless, dedicated time-dependent shrinkage measurements would be required to establish a direct quantitative relationship between evaporation kinetics and dimensional variations. Overall, most formulations recorded shrinkage values of less than 1%, indicating good dimensional stability of the material.

Fig. 11 shows the specimens mass loss during curing and the number of days required to reach stability, respectively. Specimen mass loss indicates the quantity of water that is lost during the curing phase until a constant mass is reached; this is then recorded as the number of days to reach that stability.

It is resulted that mortars containing sand showed the lowest mass loss and reached equilibrium faster than those with recycled aggregates. In particular, samples with MS showed the highest loss and the longest stabilization time, especially in the intermediate grain sizes 1.00-2.00 mm and 2.00-4.00 mm. This behaviour is likely attributable to the higher porosity or different hygroscopic behaviour of the material compared to sand-based specimens. Mortars containing CS and OS showed an intermediate behaviour, with a gradual increase in both water loss and time required to reach stability, resulting in greater residual water availability at the end of curing. These data confirmed that replacing sand with waste shells significantly alters the hygrometric behaviour of mortars, affecting water retention and stabilization time.

Optical microscope observations (Fig. 12A–D) on mortars sectioned samples highlighted significant differences in the distribution and interaction between cement matrix and waste aggregates, depending on the material used. In mortars with natural sand (Fig. 12A), the aggregate resulted uniformly distributed within the matrix, giving homogeneity to the overall compound. In fact, the cut surface appeared free of evident macro-pores and cracks, with the aggregates well integrated and clearly visible. A similar behaviour was found for mortars containing OS. As observed in the morphological analysis of the aggregates (Figs. 6 and 7), OS presents a more irregular and rough surface texture, which promotes adhesion with the cement paste and an effective incorporation of the recycled material. In addition, this behaviour is consistent with the higher specific surface area values previously reported for OS, which further enhance binder–aggregate interaction. Although no direct measurements of surface roughness or bond strength were performed, these characteristics may have contributed to the interaction between the aggregate and the cement paste. In particular, in the sample with grain size 0.00–4.00 mm (Fig. 12D), the variety of grain shapes and sizes may have contributed to a greater saturation and cohesion of the cement matrix.

On the contrary, mortars containing CS (Fig. 12C) in the same grain size fraction showed some structural irregularities. On the cut surfaces, indeed, evident voids and crystalline formations between the grains were observed, indicating a lower integration in the matrix between aggregate and binder.

The mortars with MS were distinguished by a less favorable behaviour. The cut surfaces showed numerous porosities and inhomogeneities, and the aggregate resulted poorly distributed within the cement matrix. This led to the formation of many voids, reducing the compactness and potentially the resistance of the produced material. In particular, for the grain size 0.00–4.00 mm (Fig. 12B), aggregate detachments and the presence of larger voids were evident compared to the other analysed samples.

The behaviour towards water is shown in Fig. 13A (imbibition) and Fig. 13B (capillary action). It can be observed that all the shell-based mortars presented higher values of water imbibition in comparison to the reference one.

In particular, OS-based mortars exhibited the highest water imbibition values (13.99%), followed by MS-based mortars (13.42%), while CS-based mortars showed values (10.38%) comparable to the reference mortar (10.47%). That difference could be attributed to the fact that the type of waste (mollusk) aggregate taken into consideration were more hygroscopic, compared to the sand, resulting in a greater propensity of the material to absorb water molecules. This can be further explained as these shell-based mortars resulted less dense than the reference material (cf. Fig. 8B, bulk density) hence the specimens probably resulted more porous, causing more water to be absorbed and retained inside. Such observed behaviour is in accordance with other studies found in literature (Safi et al., 2015) where the use of seashells as aggregate in mortars' manufacture led to an increased water sorptivity.

The capillary action, on the other hand, showed a more interesting behaviour. In Fig. 13B, it can be observed that with the same granulometric fraction, the capillarity index tended to decrease significantly for the shell-based samples compared to the reference material. Although shell-based mortars exhibited higher water imbibition values, their capillary absorption remained lower than that of the reference mortar. This behaviour suggests that the mechanisms governing water uptake under full immersion differ from those controlling capillary transport, resulting in different responses for the two tests. In general, it was observed that for all the granulometric fractions, the values resulted all below the value of the reference samples, demonstrating that a total substitution of sand with mollusk shells into cement mortars, lead to a considerable lower capillary absorption. That is in agreement with the results reported in (Martínez-García et al., 2019a) where a partial substitution of sand with shells led to a substantial capillary uptake decrease, with the main difference that in this novel study the sand vs shells substitution was complete. Overall, the measured capillary absorption values indicate that the incorporation of mollusk shell aggregates did not compromise the suitability of the mortars from the point of view of water transport properties, although the final applicability of each formulation should also consider its mechanical and durability performance.

It should be noted that no direct porosity characterization techniques, such as mercury intrusion porosimetry (MIP) or BET analysis, were performed in this study. Therefore, the discussion regarding porosity throughout the manuscript is based on the comparative results obtained from the water absorption by imbibition and capillary absorption tests, which provide an indirect assessment of the accessible pore network and pore connectivity of the investigated mortars rather than absolute porosity values or pore size distribution.

The mechanical performance of the specimens was assessed at 28 days of curing, and is presented in Fig. 14A and B that shows the bending resistance (BR) and the uniaxial compressive strength (UCS), respectively. It was observed that the BR of shell-based mortars decreased with increasing grain size. The highest values were recorded for samples containing OS, in the grain fractions 0.00-1.00 mm and 0.00-4.00 mm. In addition, it is interesting to note how, with the same grain size, the OS- and CS-based formulations exhibited a higher BR than the reference material. In particular, for the calibrated 0.00–4.00 mm grain size range, the OS-based mortar achieved a flexural strength of 9.15 MPa compared to 4.04 MPa for the reference mortar, corresponding to an increase of approximately 126%. This behaviour suggests that, under the investigated conditions, the replacement of natural sand with OS shell aggregates can contribute to improving the flexural performance of the mortar. Although OS-based mortars exhibited lower bulk density than the reference material, their mechanical performance was significantly higher. This indicates that density alone cannot explain the observed behaviour. The irregular and multilayered morphology of OS particles, together with the improved packing observed for the 0.00–4.00 mm fraction, may have promoted a more effective aggregate–matrix interaction, partially compensating for the density reduction and contributing to the enhanced mechanical strength. The same was observed for UCS: the highest values were recorded for OS-based mortars. In particular, for the granulometric fractions 0.00-1.00 mm and 0.00-4.00 mm a higher compressive strength of 80% and 90% respectively, than the reference material, was calculated.

The same cannot be said for MS-based mortars because they presented much less resistance, both BR and UCS, in comparison to the standard reference mortar. That is probably caused by the MS irregular, flat and sharp shape that cannot assure a proper friction within the binder paste, making the mortar weaker. That is also in accordance with the optical microscopy and SEM (cf. Figs. 6 and 7) and, at the same time, they resulted also less denser and more porous. It should also be considered that the reference aggregate consisted of a predominantly siliceous river sand, whereas the shell aggregates were mainly composed of calcium carbonate, as confirmed by the XRF and XRD analyses. This mineralogical difference may have influenced the aggregate–paste interaction and the characteristics of the interfacial transition zone (ITZ), contributing to the different mechanical behaviour observed among the investigated mortars.

The obtained findings resulted also in line with the studies of (Martínez-García et al., 2019b, 2020b) where MS was reused as fine and coarse aggregate in aerial lime mortars manufacture for coating applications. In these studies, the irregular morphology of MS particles created pores in the mortar, making it less dense and more porous, reducing the bond with the binder and compromising the final mechanical strength.

Many studies have already shown that shell-based aggregates tend to reduce the mechanical performance of materials, mainly due to the smooth surface of shells (Safi et al., 2015; Yoon et al., 2004) Our study confirmed this trend as far as MS is concerned, showing that their reuse could actually compromise the mechanical resistance of the produced mortars, a crucial factor to consider when developing new construction materials. However, it is important to note that this reduction did not apply to CS- and OS-based mortars, which showed significantly higher mechanical strength values.

UCS values of all the formulations are reported in Table 4, along with the relative classes of resistance in accordance with EN 998-1 (plastering application) (UNI EN 998-1, 2016) and EN 998-2 (masonry application) (UNI EN 998-2, 2016).

It is observed that, of all the formulations tested, CS 0.00-1.00 mm, OS 0.00-4.00 mm, and 0.00-1.00 mm are suitable as structural mortars for concrete applications (class M > 10). On the other hand, it is noted that none of the MS-based mixes are suitable as structural mortars for concrete applications, in accordance to the above discussion, while they result adequate for light structures or bed joints, with the exception of MS 1.00-2.00 mm whose UCS is too low to be considered for any application in construction. That consideration resulted highly interesting as the investigation conducted so far would allow to predict some light structural applications also for mollusk shells reuse in construction and do not discard them *a priori*. On the other hand, all the produced MS-based mixes result highly suitable for plastering/coating applications, as underlined by previous studies (Leone et al., 2023; Martínez-García et al., 2019b, 2020b).

Finally, the produced materials energy-saving performance was quantified measuring the thermal conductivity (λ) that returns the heat flow through the material. The measured λ values are presented in Fig. 15. In general, it is observed that all the developed shell-based mortars presented a lower λ in comparison to the reference mortar. In particular, among the waste-based materials, the calibrated MS 0.00-4.00 mm mix showed the highest value with a reduction of about 40% to the reference material. The lowest λ value was measured for OS 1.00-2.00 mm with nearly 60% reduction. That is explainable by the porous and light nature of the mollusk shells that, in contrast to the more compact and dense sand, acts as a sort of light aggregate, hence with a more insulating performance that is transferred to the developed mortar 95% (EN 1745:2020, 2020).

5. Preliminary evaluation of durability

Assessing durability is essential for predicting the long-term behaviour of innovative materials, especially when unconventional aggregates, such as the considered mollusk shells, are used. These materials, derived from organic waste, may have greater porosity, compositional variability, and greater susceptibility to degradation phenomena, such as water absorption, salt crystallization, or thermal alteration (Chen et al., 2023; Martínez-García et al., 2019a). For this reason, as pointed out by Tam and Tam. (2006) and Saeli et al. (2019), it is essential to supplement initial mechanical tests with specific durability tests to ensure the reliability of the material over time.

To this end, two main types of accelerated aging tests were

Table 4
UCS values for each mortar and relative class of resistance.

aggregate nature	UCS [MPa]	EN 998-2 (masonry)	EN 998-1 (plaster)
Ref. (sand 0.00-4.00 mm)	12.48 ± 0.99	M10	CSIV
Ref. (sand 0.00-1.00 mm)	10.05 ± 0.51	M10	CSIV
Ref. (sand 1.00-2.00 mm)	8.74 ± 0.78	M5	CSIV
Ref. (sand 2.00-4.00 mm)	10.51 ± 0.36	M10	CSIV
MS (0.00-4.00 mm)	3.15 ± 0.18	M2.5	CSII
MS (0.00-1.00 mm)	5.95 ± 0.09	M5	CSIII
MS (1.00-2.00 mm)	2.04 ± 0.39	M1	CSI
MS (2.00-4.00 mm)	3.11 ± 0.02	M2.5	CSII
CS (0.00-4.00 mm)	8.68 ± 1.26	M5	CSIV
CS (0.00-1.00 mm)	10.52 ± 0.48	M10	CSIV
CS (1.00-2.00 mm)	5.55 ± 0.48	M5	CSIII
CS (2.00-4.00 mm)	8.27 ± 0.42	M5	CSIV
OS (0.00-4.00 mm)	19.56 ± 0.68	M15	CSIV
OS (0.00-1.00 mm)	17.63 ± 0.41	M15	CSIV
OS (1.00-2.00 mm)	8.57 ± 0.38	M5	CSIV
OS (2.00-4.00 mm)	9.46 ± 0.26	M5	CSIV

conducted: salt crystallization test (under NaCl affection) and exposure to high thermal loads (up to 800 °C). These conditions were aimed to simulate the exposure to marine environment and salty attack in general, and events of fire or prolonged thermal stress, respectively, which are frequently encountered in real-world contexts. The choice of these tests was based on methodologies established in scientific literature and regulatory standards for assessing the resistance to degradation of cementitious materials (Galanaki et al., 2022; Nogueira et al., 2020; Bai et al., 2021; Kim et al., 2022; Martins et al., 2024).

The formulations subjected to durability testing are restricted to those with a particle size of 0.00–4.00 mm, being analogous to the granulometry of the common commercial sand for mortars. The presented results, therefore, constitute an initial assessment of the behaviour of the produced materials in extreme environmental conditions and lay the foundations for future regulatory validation and real-scale application, especially in coastal or thermally hazardous contexts.

5.1. Durability test in a saline environment

In order to conduct accelerating aging test on the selected specimens, samples were subjected to 30 cycles of salt crystallization to evaluate the resistance to degradation. To this end, NaCl was dissolved at 4% concentration in potable water to reproduce the average sea salinity. Although not intended to reproduce the full complexity of long-term marine exposure, the adopted protocol provided an accelerated comparative assessment of the resistance of the investigated mortars to salt crystallization phenomena under controlled laboratory conditions. Fig. 16 shows the experimental procedure.

As already said, the tested formulations were MS, CS, and OS in the granulometric range of 0.00-4.00 mm, to be compared to standard reference mortar (sand). Table 5 shows the visual evolution of the specimens surface/appearance at the 0th, 10th, 20th, and 30th cycle, representing the steps when the main changes were observed. In particular, it was noted that at the initial state, samples appeared compact, with small holes, except those with MS and CS, which showed higher porosity and lower homogeneity. After 10 cycles, the surface started to become rougher, with evident voids and visible exposed aggregates due to deterioration of the cement matrix. At the 20th cycle, the first salt efflorescence appeared, particularly along the edges of the specimens. Degradation advanced, especially in MS specimens, where the increased presence of voids promoted salt ingress and the formation of internal microfractures. By the end of the 30th cycle, efflorescence was widespread and high material loss was noted. That was particularly evident for MS-based mortars, which showed erosion, detachment, and color changes due to salt crystallization in the structure. In general, mortars with sand showed less degradation, due to their greater compactness and lower porosity, which limited salt ingress and improved adhesion between matrix and aggregate.

During the durability test in saline environment, all tested samples

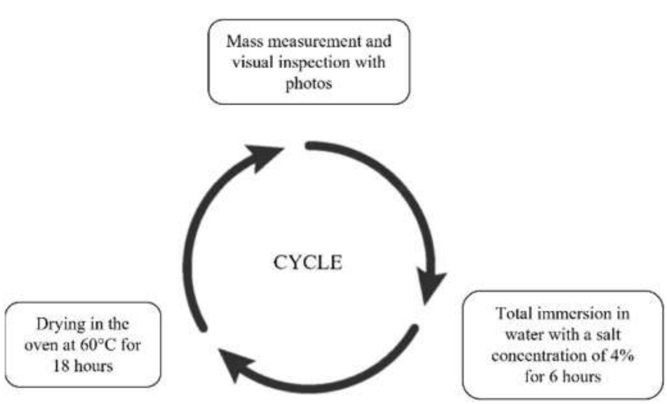

Fig. 16. Experimental procedure of the durability test in NaCl environment.

underwent considerable changes in mass. In particular, it was noted that during the first 20 cycles, the samples underwent an increase in mass due to the crystallization of NaCl salts into the mortar matrix. However, from the 20th to 30th cycle, due to the deterioration of the cement matrix and the consequent detachment of the aggregate, a slight mass loss was observed. Therefore, in Fig. 17 it is reported the total mass loss, expressed as a percentage, suffered by the samples, at the end of the 30th cycle. The highest value of mass loss was reached by OS-based mortar 0.00-4.00 mm, while the MS- and CS-based samples showed similar behaviour to reference mortar with natural bench aggregate.

The obtained results confirmed what has also been observed in the literature, namely that the resistance of mortars to salt crystallization depends heavily on the microstructure and type of aggregate used. Recent studies showed that lime-based mortars with high porosity and suboptimal pore distribution exhibit more pronounced degradation, in line with what it was found in this study for the finer and more porous formulations. In particular, Nogueira et al. (2020) demonstrated that the position of the drying front directly affects the type of crystallization and the generated damage, confirming the greater vulnerability of mortars with salt accumulation behaviour. Lubelli et al. (2006) and Hwang et al. (2022) also emphasized the importance of mortar composition and pore distribution to increase resistance to salt cycles, aspects consistent with the degradation phenomena observed in the presented tests.

5.2. Durability test under thermal loads

Durability test under thermal loads was performed to simulate the mechanical resistance of the selected mortars to fires or strong heat. Fig. 18 shows the experimental procedure followed.

Also for this test, the tested formulations were MS, CS, and OS 0.00-4.00 mm and the relative reference mortar (sand). That, once again, permitted to evaluate the resistance of mortars - in this case to heat - analogous to a building material produced with standard commercial sand. The testing samples were exposed to temperatures of 100 °C, 200 °C, 400 °C, 600 °C, and 800 °C, for a length of 1 h, following commonly adopted procedures reported in the literature (Kim et al., 2022; Martins et al., 2024). At the end of each test, the mass loss (Fig. 19A) and the compressive strength (Fig. 19B) of each mix were evaluated.

Fig. 19A shows the mass loss of specimens caused to prolonged heat exposure. It is observed an increasing mass loss as the exposing temperature was increased. At 100 °C, the mass loss resulted about 1%, with similar values among the different shell types and the reference sand. At 600 °C, samples with recycled aggregate showed a mass loss between 5% and 7%, which is higher than that of the reference (sand) mortar. At 800 °C, MS specimens destroyed completely, while CS mortars showed a loss of up to 16%. At 800 °C, OS mortars showed a mass loss of about 13–14%, exhibiting a progressive degradation but without the structural collapse observed in the MS specimens. This behaviour suggests a different thermal stability of the investigated shell aggregates and their interaction with the cement matrix. From a practical point of view, the results indicate that OS-based mortars retained a residual integrity under extreme thermal exposure, whereas MS-based mortars may present limitations in applications where severe fire or high-temperature resistance is required.

Fig. 19B shows the uniaxial compressive strength of the mortars after each cycle of heat aging. It resulted that, compared to the original UCS measured at ambient conditions (20 ± 2 °C), fired samples showed a progressive decrease in strength with increasing exposure temperature. In particular, from 100 °C to 400 °C, a moderate decrease was observed for all the analysed samples. When the temperature reached 600 °C, a drastic reduction in strength was observed in the shell-based samples, especially in MS, which recorded values close to 0 MPa – complete destruction under minimal loads. Of all the shell aggregates analysed, OS mortars exhibited the highest residual strength after exposure to 800 °C. While the reference mortar reached 0 MPa, OS mortars retained

Table 5
Photographs of the specimens collected during the salt crystallization durability test at different exposure cycles. All specimens had dimensions of 40 × 40 × 160 mm.

Cycles	Sand	MS	CS	OS
0				
10				
20				
30				

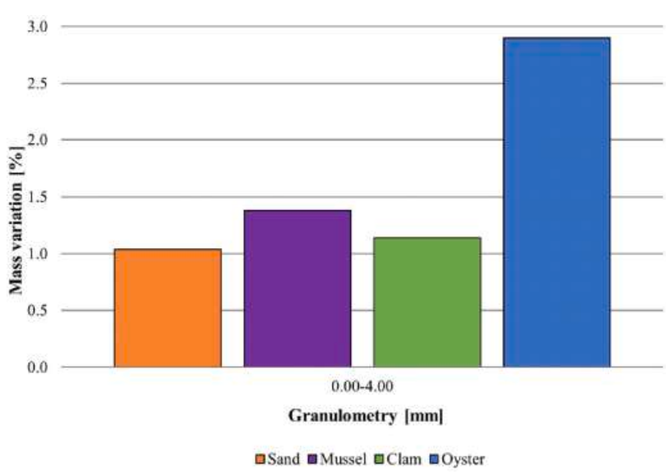

Fig. 17. Mass variation [%] following durability test in a saline environment, after 30 aging cycles.

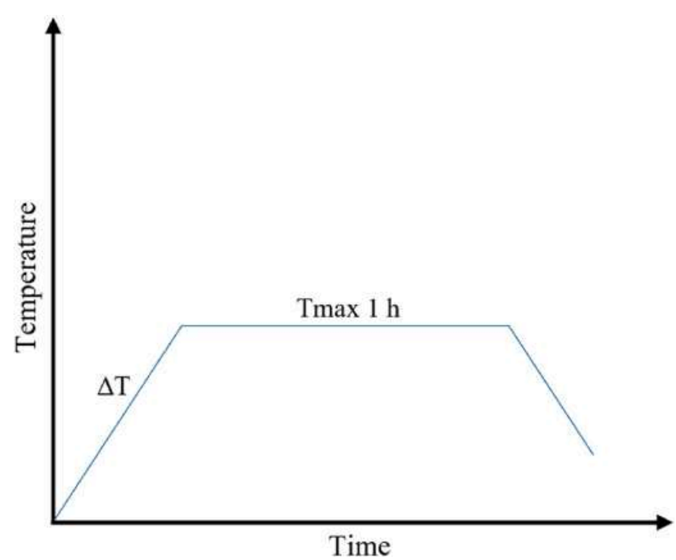

Fig. 18. Experimental procedure of the durability test under thermal loads.

a residual strength of approximately 2 MPa. Although this value is very low in absolute terms, it suggests a greater resistance to thermal degradation compared to the other formulations tested.

These results are consistent with the literature. Kim et al. (2022) reported that, for OPC-based materials, an exposure to high temperatures caused severe cracking and a significant drop in mechanical properties, mainly due to the decomposition of cement hydration products, in particular C-S-H (calcium silicate hydrate). According to the authors, three main degradation phases can be identified: (1) the dehydration of ettringite and loss of capillary water (100-300 °C); (2) the decomposition of calcium hydroxide (400-500 °C); and (3) the decomposition of calcium carbonate (600-800 °C). These sequential transformations lead to an increase in porosity, an ignition of the carbon fractions, and a complete loss of structural bonds in the cement matrix, resulting in increased permeability and crack propagation. In addition, the rapid evaporation of the residual trapped water could contribute in causing further internal pressure to cracking. As also observed by Martins et al. (2024) ovens are widely used to assess the fire resistance of building materials, through heating cycles followed by mechanical tests (as in the present study and those of Bamonte et al. (2021), Cülfik e Özturan (2002), Djaknoun et al. (2012) and Pachta et al. (2018). However, for technical and economic reasons, many studies did not

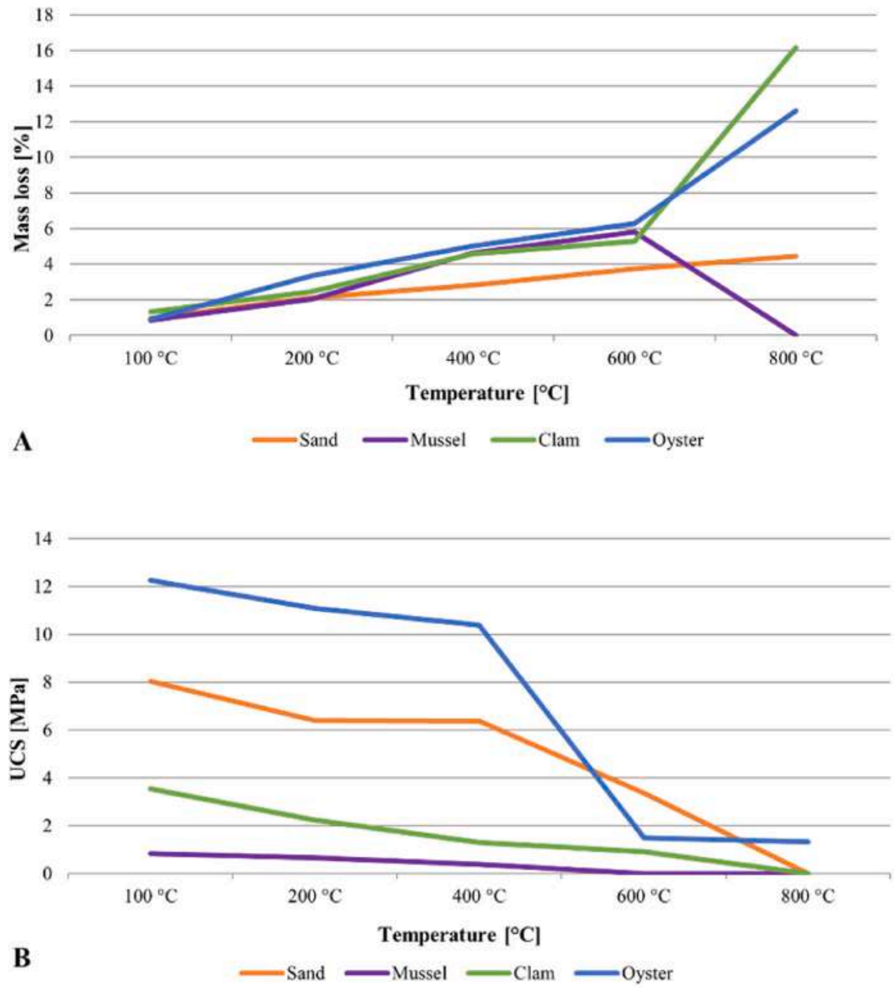

Fig. 19. Durability test under thermal loads: A) Mass loss; B) Uniaxial compressive strength.

strictly follow current standards. Among the most widely adopted procedures are those ruled by the Brazilian NBR 16965 (BNT NBR 16965, 2021), Eurocode 6 (EN, 1996-1-1, 2005), and the RILEM TC 200-HTC recommendations (RILEM TC 200, 2007), which provide guidelines for the evaluation of the fire resistance of building elements and the mechanical properties of concrete at high temperatures. In addition, ASTM C199 (ASTM C199, 2022) defines standardised methods to test the resistance of refractory mortars at elevated temperatures. However, as highlighted by Martins et al. (2024), there is a lack of specific standards for the characterisation of cladding mortars subjected to high temperatures, highlighting the need for further regulatory developments in this area.

6. Conclusions

This experimental research investigated the possibility of producing novel sustainable bio-composite mortars by fully replacing natural sand with ground mollusk shells (MS, CS, and OS) for potential applications in the construction sector. The main findings were:

- The workability of the mortars was strongly influenced by the particle size of the shells: the finest fractions (0.00–1.00 mm) significantly reduced the spread value, whereas the coarser fractions (1.00–2.00 mm; 2.00–4.00 mm) improved the mix consistency. The CS 0.00–4.00 mm formulation exhibited a workability comparable to the reference mortar, while OS 0.00–4.00 mm showed the lowest spread (10.5 cm), resulting in a non-workable mixture.
- All aggregates derived from the considered mollusks' shells resulted in a significant reduction in bulk density compared with the reference mortar. Among the formulations investigated, those based on MS exhibited the lowest density values, demonstrating interesting potential for lightweight non-structural applications.
- Mechanical performance strongly depended on the type of shell employed. OS-based mortars achieved the highest strength values, with OS 0.00–4.00 mm reaching the maximum compressive strength (19.56 MPa, +90% compared to the reference) and a flexural strength increase of about +120%. OS 0.00–1.00 mm also exhibited remarkable behaviour (17.63 MPa, +80%). Conversely, MS-based mixes provided the lowest values (minimum 2.04 MPa), although still suitable for non-structural and plastering applications.
- Water-related properties were strongly influenced by the considered mollusks' shell aggregates. All shell-based mortars exhibited higher water imbibition values than the reference mortar, particularly the OS-based formulations. Conversely, capillary absorption coefficients were consistently lower than those measured for the reference mortar, indicating different water transport mechanisms under full immersion and capillary suction conditions.
- Thermal conductivity was markedly reduced in all formulations. The OS 1.00–2.00 mm mix exhibited the greatest decrease (−60%), followed by MS 0.00–4.00 mm (−40%) and CS-based mixes (−30 to −50%), confirming their potential as lightweight insulating mortars.
- In the salt crystallization test (30 cycles), different durability behaviours were observed depending on the shell type. MS and CS showed mass losses comparable to the reference mortar, while OS

exhibited the highest mass loss, highlighting the need for further long-term investigations on the resistance of shell-based mortars to saline environments.

- Under thermal loads up to 800 °C, OS-based mortars showed the most stable behaviour, maintaining a residual compressive strength of approximately 2 MPa. MS collapsed at 600 °C, and both CS and the reference mortar reached 0 MPa at 800 °C.

Overall, most formulations produced in this study achieved compressive strength, density, and capillary absorption values suitable for various construction applications. Some OS- and CS-based mortars proved adequate even for lightweight structural applications (classes M10–M15), whereas MS-based mixes appeared more suitable for plastering and non-structural coating applications. Furthermore, all shell-based mortars exhibited lower thermal conductivity values than the traditional sand-based mortar, highlighting the potential of shell waste aggregates for the development of lightweight cementitious materials with improved thermal insulation properties. The contrasting behaviour observed among the investigated shell types appears to be strongly related to their morphological characteristics and their interaction with the cement matrix. In particular, OS aggregates exhibited the best overall mechanical performance, likely due to their irregular and multilayered surface, which promoted a more effective aggregate–matrix bond and improved particle packing. Conversely, the flatter and sharper morphology of MS particles resulted in weaker cohesion and lower mechanical strength, despite their favorable lightweight characteristics and thermal insulation performance. CS-based mortars generally showed an intermediate behaviour, combining satisfactory mechanical properties with reduced thermal conductivity. These findings highlight that the engineering performance of shell-based mortars is governed not only by density and particle size distribution, but also by the morphology of the recycled aggregates and their ability to interact with the cementitious matrix.

Furthermore, the reuse of MS, CS and OS aggregates can contribute to reducing the consumption of natural sand and promoting the valorisation of an organic by-product otherwise destined for disposal. Potential environmental and economic benefits associated with this approach should be quantified through dedicated life-cycle and techno-economic assessments. This approach is consistent with the principles of the European Circular Economy and current sustainability-oriented strategies in the construction sector.

In this preliminary study, mollusk shells were processed in various particle size ranges (0.00–1.00 mm, 1.00–2.00 mm, 2.00–4.00 mm, and a calibrated 0.00–4.00 mm blend to imitate a common sand composition), and the resulting mortars were fabricated through a simple, conventional procedure compatible with common construction-site practices. From a practical perspective, the proposed approach could be integrated into existing mortar production systems, since the required shell processing operations (cleaning, crushing, and sieving) are comparable to conventional aggregate preparation procedures. Nevertheless, large-scale implementation would require a reliable supply chain for shell waste collection, quality control protocols, and dedicated techno-economic assessments to evaluate industrial feasibility and cost-effectiveness.

Future investigations will focus a vast evaluation of long-term durability, including freeze–thaw cycles and with particular attention to carbonation phenomena and interaction with soluble salts, useful to predict strength/weakness point of application in real aggressive contexts. In addition, post-ageing microstructural and mineralogical characterisation (e.g., XRD, SEM/EDS) will be performed to better elucidate the degradation mechanisms occurring after environmental exposure and to validate the hypotheses proposed in the present study. Specific studies should address the long-term chemical durability of shell-based mortars, including chloride migration, alkali-related reactions and their potential implications for reinforced cementitious systems. Also, industrial scalability will be analysed based on life cycle assessment (LCA) and techno-economic studies to properly define real potentials and draw backs in the construction sector.

CRediT authorship contribution statement

Adriana Calà: Data curation, Formal analysis, Investigation, Writing – original draft, Writing – review & editing. **Marinélia N. Capela:** Formal analysis, Investigation, Writing – original draft, Writing – review & editing. **Rosanna Leone:** Formal analysis, Investigation, Writing – original draft. **Simona Colajanni:** Supervision, Writing – original draft. **Tiziana Campisi:** Supervision, Writing – original draft. **Manfredi Saeli:** Data curation, Formal analysis, Methodology, Supervision, Validation, Writing – original draft, Writing – review & editing.

Author contributions

The state of the art and the literature review was conducted by Adriana Calà; the experimental plan was designed by Manfredi Saeli; materials development and testing was conducted by Adriana Calà and Rosanna Leone; the waste physico-chemical analyses and discussion were conducted by Marinélia N. Capela; the discussion on mortars performance and results was conducted by Adriana Calà and Manfredi Saeli; Tiziana Campisi, Simona Colajanni, and Manfredi Saeli were in charge of the scientific coordination. All the authors were involved in the manuscript preparation and implementation.

Declaration of generative AI use

The authors declared that generative AI was not used in this study.

Funding

This research did not receive any specific grant from funding agencies in the public, commercial, or not-for-profit sectors.

Declaration of competing interests

The authors declare that they have no known competing financial interests or personal relationships that could have appeared to influence the work reported in this paper.

Acknowledgements

The Company S.A.C.O.M. srl, based in Messina (Italy), is thanked for the furniture of mollusk shells. This work was developed within the scope of the project CICECO Aveiro Institute of Materials, UID/50011/2025 (DOI 10.54499/UID/50011/2025) & LA/P/0006/2020 (DOI 10.54499/LA/P/0006/2020), financed by national funds through the FCT/MCTES (PIDDAC).

This study was developed in the framework of the research activities carried out within the Project "Network 4 Energy Sustainable Transition — NEST", Spoke 8: Final use optimization, sustainability & resilience in energy supply chain, Project code PE0000021, Concession Decree No. 1561 of 11.10.2022 adopted by Ministero dell'Università e della Ricerca (MUR), CUP B73C22001280006. Project funded under the National Recovery and Resilience Plan (NRRP), Mission 4 Component 2 Investment 1.3 - Call for tender No. 341 of 15.03.2022 of MUR; funded by the European Union – NextGenerationEU.

Data availability

Data will be made available on request.

References

ACI 116R-00, 2000. Cement and Concrete Terminology, 116. American Concrete Institute (ACI) Committee, Farmington Hills, MI, USA.

Alonso, A.A., Álvarez-Salgado, X.A., Antelo, L.T., 2021. Assessing the impact of bivalve aquaculture on the carbon circular economy. J. Clean. Prod. 279, 123873. https://doi.org/10.1016/j.jclepro.2020.123873.

ASTM C199, 2022. Standard Test Method for Pier Test for Refractory Mortars. ASTM International, West Conshohocken, PA.

Bai, L., Xie, J., Liu, J., Xie, Y., 2021. Effect of salt on hygroscopic properties of cement mortar. Constr. Build. Mater. 305, 124746. https://doi.org/10.1016/j.conbuildmat.2021.124746.

Bamonte, P.G., Gambarova, F., Sciarretta, F., 2021. Thermo-mechanical properties and stress–strain curves of ordinary cementitious mortars at elevated temperatures. Constr. Build. Mater. 267, 121027. https://doi.org/10.1016/j.conbuildmat.2020.121027.

Bhatti, I.A., Lee, J., Jang, Y.-D., Kim, K.-S., Kwon, J.-H., 2008. Analysis of shellfish by thermoluminescence and X-ray diffraction methods: knowledge of gamma-ray treatment and mineral characterization. Radiat. Phys. Chem. 77, 663–668. https://doi.org/10.1016/j.radphyschem.2007.12.009.

BNT NBR 16965, 2021. Fire Resistance Tests for Elements of Building construction—General Guidance. Brazilian Association for Technical Standards (ABNT), Rio de Janeiro.

Caroscio, L., De Pascale, B., Tataranni, P., Chiavetta, C., Lantieri, C., Bonoli, A., 2024. Preliminary study on the application of waste bivalve shells as biofiller for the production of asphalt concrete. Clean. Eng. Technol. 20, 100743. https://doi.org/10.1016/j.clet.2024.100743.

Checa, A.G., Jiménez-López, C., Rodríguez-Navarro, A., Machado, J.P., 2007. Precipitation of aragonite by calcitic bivalves in Mg-enriched marine waters. Mar. Biol. 150, 819–827. https://doi.org/10.1007/s00227-006-0411-4.

Chen, B., Peng, L., Zhong, H., Zhao, Y., Meng, T., Zhang, B., 2023. Synergetic recycling of recycled concrete aggregate and waste mussel shell in concrete: mechanical properties, durability and microstructure. Constr. Build. Mater. 371, 130825. https://doi.org/10.1016/j.conbuildmat.2023.130825.

Chen, Z., Tang, Y., Mai, C., Shi, J., Xie, Y., Hu, H., 2020. Experimental study on the shear performance of brick masonry strengthened with modified oyster shell ash mortar. Case Stud. Constr. Mater. 13, e00469. https://doi.org/10.1016/j.cscm.2020.e00469.

Cintura, E., Nunes, L., Esteves, B., Faria, P., 2021. Agro-industrial wastes as building insulation materials: a review and challenges for Euro-Mediterranean countries. Ind. Crops Prod. 171, 113833. https://doi.org/10.1016/j.indcrop.2021.113833.

Cülfik, M.S., Özturan, T., 2002. Effect of elevated temperatures on the residual mechanical properties of high-performance mortar. Cem. Concr. Res. 32, 809–816. https://doi.org/10.1016/S0008-8846(02)00709-3.

Dassori, E., Morbiducci, R., 2020. Costruire l'architettura. Tecniche E Tecnologie per il Progetto, second ed. Tecniche Nuove, Milan.

De Pascale, B., Tarsi, G., Tataranni, P., Sangiorgi, C., 2024. Potential application of waste bivalve shells as recycled filler in porous asphalt concrete through rheo-mechanical analysis. Resour. Conserv. Recycl. 209, 107830. https://doi.org/10.1016/j.resconrec.2024.107830.

Djaknoun, E., Ouedraogo, A.A., Benyahia, A., 2012. Characterisation of the behavior of high performance mortar subjected to high temperatures. Constr. Build. Mater. 28, 176–186. https://doi.org/10.1016/j.conbuildmat.2011.07.063.

EN 1745:2020, 2020. Masonry and Masonry Products – Methods for Determining Thermal Properties. European Committee for Standardization (CEN), Brussels, Belgium.

EN 1992-1-1, 2004. Eurocode 2: Design of Concrete structures—Part 1-1: General Rules and Rules for Buildings. European Committee for Standardization (CEN), Brussels (amended 2014).

EN 1996-1-1, 2005. Eurocode 6: Design of Masonry structures—Part 1-1: General Rules for Reinforced and Unreinforced Masonry Structures. European Committee for Standardization (CEN), Brussels.

European Commission, 2024. Directorate-general for maritime affairs and fisheries. Fish names database. https://fish-commercial-names.ec.europa.eu/fish-names/home_en. (Accessed 25 March 2026).

European Council of the European Union, 2024. Circular economy. https://www.consilium.europa.eu/en/policies/circular-economy/. (Accessed 2 August 2025).

European Market Observatory for Fisheries and Aquaculture Products (EUMOFA), 2022a. Case Study: Mussel in the EU. Publications Office of the European Union, Luxembourg. https://doi.org/10.2771/855734.

European Market Observatory for Fisheries and Aquaculture Products (EUMOFA), 2022b. Oysters in the EU: Price Structure in the Supply Chain – Focus on France, Ireland and the Netherlands. Publications Office of the European Union, Luxembourg.

European Market Observatory for Fisheries and Aquaculture Products (EUMOFA), the EU Fish Market, 2025. Publications Office of the European Union, Luxembourg.

European Parliament, 2024. Directorate-general for communication, Green Deal: key to a climate-neutral and sustainable EU. https://www.europarl.europa.eu/pdfs/news/expert/2022/6/story/20200618STO81513/20200618STO81513_en.pdf. (Accessed 2 August 2025).

European Parliament and Council, 2009. Regulation (EC) No 1069/2009 of 21 October 2009 laying down health rules as regards animal by-products not intended for human consumption and repealing Regulation (EC) No 1774/2002. Off. J. Eur. Union L 300, 1–33.

Ez-zaki, H., El Gharbi, B., Diouri, A., 2018. Development of eco-friendly mortars incorporating glass and shell powders. Constr. Build. Mater. 159, 198–204. https://doi.org/10.1016/j.conbuildmat.2017.10.125.

FAO, 2022. Cultured Aquatic Species Information Programme – Mytilus galloprovincialis. FAO Fisheries Division, Rome. https://www.fao.org/fishery/en/culturedspecies/mytilus_galloprovincialis. (Accessed 25 March 2026).

FAO, 2024. The State of World Fisheries and Aquaculture 2024. FAO, Rome. https://doi.org/10.4060/cc0461en.

Galanaki, N., Delegou, E., Bris, T., Moropoulou, A., 2022. Accelerated ageing tests of sodium chloride for the evaluation of stones durability to salt crystallization: a comparative study of selected restoration lithotypes. Dev. Built Environ. 11, 100081. https://doi.org/10.1016/j.dibe.2022.100081.

Ghaffar, S., Corker, J., Fan, M., 2018. Additive manufacturing technology and its implementation in construction as an eco-innovative solution. Autom. Constr. 93. https://doi.org/10.1016/j.autcon.2018.05.005.

González-Caro, Á., Merino-Lechuga, A.M., Suescum-Morales, D., Fernández-Ledesma, E., Fernández-Rodríguez, J.M., Jiménez, J.R., 2025. Performance of self-compacting mortars using ground seashells as recycled sand. Materials 18 (2), 418. https://doi.org/10.3390/ma18020418.

Gosling, E., 2015. Bivalve Molluscs: Biology, Ecology and Culture, second ed. Wiley-Blackwell, Oxford.

Harper, E.M., 2000. Are calcitic layers an effective adaptation against shell dissolution in the Bivalvia? J. Zool. 251, 179–186. https://doi.org/10.1111/j.1469-7998.2000.tb00602.x.

Hwang, H.-Y., Kwon, Y.-H., Hong, S.-G., Kang, S.-H., 2022. Comparative study of effects of natural organic additives and cellulose ether on properties of lime-clay mortars. J. Build. Eng. 48, 103972. https://doi.org/10.1016/j.jobe.2021.103972.

Islam, M.R., Ishiguro, S., Yamanaka, M., 2015. Surface heat reduction of asphalt concrete by top filling with mortar prepared by oyster shell aggregate and ground granulated blast furnace slag and their strength in different curing condition. Trans. Jpn. Soc. Irrig. Drain. Rural Eng. 83, I_1–I_7. https://doi.org/10.11408/jsidre.83.I_1.

Italian Ministry of Infrastructure and Transport (MIT), 2018. Ministerial Decree 17 January 2018—Norme Tecniche per le Costruzioni (NTC 2018), Off. Gaz. Ital. Repub., No. 42, 20 February 2018, Ordinary Supplement No. 8. https://www.gazzettaufficiale.it/eli/id/2018/02/20/18A00716/sg.

Kim, H., Siddique, S., Jang, J.G., 2022. Effect of carbonation curing on the mechanical properties of belite-rich cement mortar exposed to elevated temperatures. J. Build. Eng. 52, 104453. https://doi.org/10.1016/j.jobe.2022.104453.

Kobayashi, I., Samata, T., 2006. Bivalve shell structure and organic matrix. Mater. Sci. Eng. C 26, 692–698. https://doi.org/10.1016/j.msec.2005.09.101.

Leone, R., Calà, A., Capela, M.N., Colajanni, S., Campisi, T., Saeli, M., 2023. Recycling mussel shells as secondary sources in green construction materials: a preliminary assessment. Sustainability 15, 3547. https://doi.org/10.3390/su15043547.

Lertwattanaruk, P., Makul, N., Siripattarapravat, C., 2012. Utilization of ground waste seashells in cement mortars for masonry and plastering. J. Environ. Manag. 111, 133–141. https://doi.org/10.1016/j.jenvman.2012.06.032.

Liao, Y., Wang, X., Wang, L., Yin, Z., Da, B., Chen, D., 2022. Effect of waste oyster shell powder content on properties of cement-metakaolin mortar. Case Stud. Constr. Mater. 16, e01088. https://doi.org/10.1016/j.cscm.2022.e01088.

Lubelli, B., van Hees, R.P.J., Huinink, H.P., Groot, C.J.W.P., 2006. Irreversible dilation of NaCl contaminated lime–cement mortar due to crystallization cycles. Cem. Concr. Res. 36, 678–687. https://doi.org/10.1016/j.cemconres.2005.10.008.

Luo, K., Zhang, M., Jiang, Q., Wang, S., Zhuo, X., 2024. Evaluation of using oyster shell as a complete replacement for aggregate to make eco-friendly concrete. J. Build. Eng. 84, 108587. https://doi.org/10.1016/j.jobe.2024.108587.

Martínez-García, C., González-Fonteboa, B., Carro-López, D., Martínez-Abella, F., 2019a. Design and properties of cement coating with mussel shell fine aggregate. Constr. Build. Mater. 215, 494–507. https://doi.org/10.1016/j.conbuildmat.2019.04.211.

Martínez-García, C., González-Fonteboa, B., Carro-López, D., Martínez-Abella, F., 2019b. Impact of mussel shell aggregates on air lime mortars: pore structure and carbonation. J. Clean. Prod. 215, 650–668. https://doi.org/10.1016/j.jclepro.2019.01.121.

Martínez-García, C., González-Fonteboa, B., Carro-López, D., Martínez-Abella, F., 2020b. Effects of mussel shell aggregates on hygric behaviour of air lime mortar at different ages. Constr. Build. Mater. 252, 119113. https://doi.org/10.1016/j.conbuildmat.2020.119113.

Martínez-García, C., González-Fonteboa, B., Carro-López, D., Pérez-Ordóñez, J.L., 2020a. Mussel shells: a canning industry by-product converted into a bio-based insulation material. J. Clean. Prod. 269, 122343. https://doi.org/10.1016/j.jclepro.2020.122343.

Martínez-García, C., González-Fonteboa, B., Carro-López, D., Pérez-Ordóñez, J.L., 2021. Assessment of mussel shells building solutions: a real-scale application. J. Build. Eng. 44, 102635. https://doi.org/10.1016/j.jobe.2021.102635.

Martínez-García, C., González-Fonteboa, B., Martínez-Abella, F., Carro-López, D., 2017. Performance of mussel shell as aggregate in plain concrete. Constr. Build. Mater. 139, 570–583. https://doi.org/10.1016/j.conbuildmat.2016.09.091.

Martins, L.M., de Carvalho, J.M.F., de Oliveira, T.M., Mendes, J.C., 2024. Behavior of cement-based coating mortars under fire or high temperatures: a systematic literature review. Constr. Build. Mater. 443, 137661. https://doi.org/10.1016/j.conbuildmat.2024.137661.

Naji, A., Elsheikh, A., 2023. A review of sustainability applications in the construction industry: perspectives and challenges. Vestn. MGSU 18, 771–784. https://doi.org/10.22227/1997-0935.2023.5.771-784.

Nogueira, R., Ferreira Pinto, A.P., Gomes, A., 2020. Artificial ageing by salt crystallization: test protocol and salt distribution patterns in lime-based rendering mortars. J. Cult. Herit. 45, 180–192. https://doi.org/10.1016/j.culher.2020.01.013.

Pachta, V., Triantafyllaki, S., Stefanidou, M., 2018. Performance of lime-based mortars at elevated temperatures. Constr. Build. Mater. 189, 576–584. https://doi.org/10.1016/j.conbuildmat.2018.09.027.

RILEM TC 200-HTC, mechanical concrete properties at high temperatures: modelling and applications. Mater. Struct. 40, 2007, 855–864. https://doi.org/10.1617/s11527-007-9286-1.

Saeli, M., Senff, L., Tobaldi, D.M., Seabra, M.P., Labrincha, J.A., 2019. Novel biomass fly ash-based geopolymeric mortars using lime slaker grits as aggregate for applications in construction: influence of granulometry and binder/aggregate ratio. Constr. Build. Mater. 227, 116643. https://doi.org/10.1016/j.conbuildmat.2019.116643.

Safi, B., Saidi, M., Daoui, A., Bellal, A., Mechekak, A., Toumi, K., 2015. The use of seashells as a fine aggregate (by sand substitution) in self-compacting mortar (SCM). Constr. Build. Mater. 78, 430–438. https://doi.org/10.1016/j.conbuildmat.2015.01.009.

Shan, H.Z., Zhuo, S.J., Shen, R.X., Sheng, C., 2008. Mineralogical effect correction in wavelength dispersive X-ray fluorescence analysis of pressed powder pellets. Spectrochim. Acta B 63, 612–616. https://doi.org/10.1016/j.sab.2008.03.004.

Silva, T.H., Mesquita-Guimarães, J., Henriques, B., Silva, F.S., Fredel, M.C., 2019. The potential use of oyster shells as a raw material for the production of new value-added products. Resources 8, 13. https://doi.org/10.3390/resources8010013.

Smaal, A.C., Ferreira, J.G., Grant, J., Petersen, J.K., Strand, Ø., 2019. Goods and Services of Marine Bivalves. Springer, Cham. https://doi.org/10.1007/978-3-319-96776-9.

Tam, V.W.Y., Tam, C.M., 2006. A review on the viable technology for construction waste recycling. Resour. Conserv. Recycl. 47, 209–221. https://doi.org/10.1016/j.resconrec.2005.12.002.

Tsang, Y.F., Kumar, V., Samadar, P., Yang, Y., Lee, J., Ok, Y.S., Song, H., Kim, K.-H., Kwon, E.E., Jeon, Y.J., 2019. Production of bioplastic through food waste valorization. Environ. Int. 127, 625–644. https://doi.org/10.1016/j.envint.2019.03.076.

UNI EN 1008, 2003. Mixing Water for concrete—Specification for Sampling, Testing and Assessing the Suitability of Water, Including Water Recovered from Processes in the Concrete Industry. European Standard, Brussels.

UNI EN 12667, 2002. Thermal Performance of Building Materials and products—Determination of Thermal Resistance by Means of Guarded Hot Plate and Heat Flow Meter methods—Products of High and Medium Thermal Resistance. European Standard, Brussels.

UNI EN 13139, 2013. Aggregates for Mortars, European Standard, Brussels.

UNI EN 1015-18, 2004. Methods of Test for Mortar for masonry—Determination of Water Absorption Coefficient due to Capillary Action of Hardened Mortar. European Standard, Brussels.

UNI EN 1015-11, 2019. Methods of Test for Mortar for masonry—Part 11: Determination of Flexural and Compressive Strength of Hardened Mortar. European Standard, Brussels.

UNI EN 1015-3, 1999. Methods of Test for Mortar for masonry—Part 3: Determination of Consistence of Fresh Mortar (By Flow Table). European Standard, Brussels.

UNI EN 197-1, 2011. Cement—Part 1: Composition, Specifications and Conformity Criteria for Common Cements, European Standard, Brussels.

UNI EN 196-1, 2016. Methods of Testing cement—Part 1: Determination of Strength, European Standard, Brussels.

UNI EN 998-1, 2016. Specification for Mortar for masonry—Part 1: Rendering and Plastering Mortar. European Standard, Brussels.

UNI EN 998-2, 2016. Specification for Mortar for masonry—Part 2: Masonry Mortar. European Standard, Brussels.

United Nations, 2015. Transforming our world: the 2030 agenda for sustainable development. Resolution Adopted by the General Assembly on 25 September 2015 (A/RES/70/1). United Nations, New York. https://www.un.org/en/development/desa/population/migration/generalassembly/docs/globalcompact/A_RES_70_1_E.pdf. (Accessed 2 August 2025).

United Nations Environment Programme, 2023. Building Materials and the Climate: Constructing a New Future. UNEP, Nairobi.

United Nations Environment Programme, 2024. Food waste index report 2024: think eat save – tracking progress to halve global food waste. https://wedocs.unep.org/20.500.11822/45230. (Accessed 2 August 2025).

Yao, Z.T., Xia, M.S., Li, H., Chen, T., Ye, Y., Zheng, H., 2014. Bivalve shell: not an abundant useless waste but a functional and versatile biomaterial. Crit. Rev. Environ. Sci. Technol. 44, 2502–2530. https://doi.org/10.1080/10643389.2013.829763.

Yoon, G.-L., Kim, B.-T., Kim, B.-O., Han, S.-H., 2003. Chemical–mechanical characteristics of crushed oyster shell. Waste Manag. 23, 825–834. https://doi.org/10.1016/S0956-053X(02)00159-9.

Yoon, H., Park, S., Lee, K., Park, J., 2004. Oyster shell as substitute for aggregate in mortar. Waste Manag. Res. 22, 158–170. https://doi.org/10.1177/0734242X04042456.